



University of Kentucky  
UKnowledge

---

Theses and Dissertations--Medical Sciences

Medical Sciences

---


2022

## APOE Genotype and Sex Modulate Ketogenic Diet Enhancements to Metabolism and Gut Microbiome in Young Mice

Andrew T. Yackzan

University of Kentucky, [andrew.t.yackzan@uky.edu](mailto:andrew.t.yackzan@uky.edu)

Author ORCID Identifier:

 <https://orcid.org/0000-0002-3426-8473>

Digital Object Identifier: <https://doi.org/10.13023/etd.2022.268>

[Right click to open a feedback form in a new tab to let us know how this document benefits you.](#)

### Recommended Citation

Yackzan, Andrew T., "APOE Genotype and Sex Modulate Ketogenic Diet Enhancements to Metabolism and Gut Microbiome in Young Mice" (2022). *Theses and Dissertations--Medical Sciences*. 21.  
[https://uknowledge.uky.edu/medsci\\_etds/21](https://uknowledge.uky.edu/medsci_etds/21)

This Master's Thesis is brought to you for free and open access by the Medical Sciences at UKnowledge. It has been accepted for inclusion in Theses and Dissertations--Medical Sciences by an authorized administrator of UKnowledge. For more information, please contact [UKnowledge@lsv.uky.edu](mailto:UKnowledge@lsv.uky.edu).

## **STUDENT AGREEMENT:**

I represent that my thesis or dissertation and abstract are my original work. Proper attribution has been given to all outside sources. I understand that I am solely responsible for obtaining any needed copyright permissions. I have obtained needed written permission statement(s) from the owner(s) of each third-party copyrighted matter to be included in my work, allowing electronic distribution (if such use is not permitted by the fair use doctrine) which will be submitted to UKnowledge as Additional File.

I hereby grant to The University of Kentucky and its agents the irrevocable, non-exclusive, and royalty-free license to archive and make accessible my work in whole or in part in all forms of media, now or hereafter known. I agree that the document mentioned above may be made available immediately for worldwide access unless an embargo applies.

I retain all other ownership rights to the copyright of my work. I also retain the right to use in future works (such as articles or books) all or part of my work. I understand that I am free to register the copyright to my work.

## **REVIEW, APPROVAL AND ACCEPTANCE**

The document mentioned above has been reviewed and accepted by the student's advisor, on behalf of the advisory committee, and by the Director of Graduate Studies (DGS), on behalf of the program; we verify that this is the final, approved version of the student's thesis including all changes required by the advisory committee. The undersigned agree to abide by the statements above.

Andrew T. Yackzan, Student

Dr. Ai-Ling Lin, Major Professor

Dr. Melinda Wilson, Director of Graduate Studies

APOE GENOTYPE AND SEX  
MODULATE KETOGENIC DIET ENHANCEMENTS  
TO METABOLISM AND GUT MICROBIOME IN YOUNG MICE

---

THESIS

---

A thesis submitted in partial fulfillment of the  
requirements for the degree of Master of Science in the  
College of Medicine  
at the University of Kentucky

By

Andrew Yackzan

Lexington, Kentucky

Director: Dr. Ai-Ling Lin, Professor of Radiology and Biological Sciences

Lexington, Kentucky

2022

Copyright © Andrew Yackzan 2022

<https://orcid.org/0000-0002-3426-8473>

## ABSTRACT OF THESIS

### APOE GENOTYPE AND SEX MODULATE KETOGENIC DIET ENHANCEMENTS TO METABOLISM AND GUT MICROBIOME IN YOUNG MICE

The apolipoprotein  $\epsilon$  (APOE) allele in humans has been associated with risk for development of Alzheimer's disease (AD). There are predominately three variations of the allele –  $\epsilon 2$  (E2),  $\epsilon 3$  (E3), and  $\epsilon 4$  (E4) – with E4 contributing the greatest risk of AD development. Recent research has unveiled evidence of neurometabolic and neurovascular deficits in E4 carriers present decades before the onset of dementia; it is believed these chronic defects play a major role in the development of AD, thus making them a potential target for preventative intervention. The purpose of this study was to examine the effect of a ketogenic diet (KD) on cerebral metabolites, gut microbiome, and cerebral perfusion in young transgenic mice carrying the E4 allele. Here we show that within 16 weeks, the control E4 female mice had the worst outcomes, while the KD significantly rescued E4 female health markers compared to the other groups.

**KEYWORDS:** Alzheimer's Disease, Apolipoprotein  $\epsilon$ , Ketogenic Diet, APOE Target-replacement (APOE-TR), gut microbiome, neurodegenerative disease.

---

Andrew Yackzan

*(Name of Student)*

---

04/05/2022

Date

APOE GENOTYPE AND SEX  
MODULATE KETOGENIC DIET ENHANCEMENTS  
TO METABOLISM AND GUT MICROBIOME IN YOUNG MICE

By  
Andrew Yackzan

Dr. Ai-Ling Lin

---

Director of Thesis

Dr. Melinda Wilson

---

Director of Graduate Studies

05/05/2022

---

Date

To my parents and committee members, who have inspired, encouraged, and supported me through this process. Thank you.

## ACKNOWLEDGMENTS

The following thesis, while an individual work, benefited from the insights and direction of several people. First, my Thesis Chair, Dr. Ai-Ling Lin, has been an incredible mentor, exemplifying the high-quality scholarship to which I aspire. In addition, I wish to thank my Thesis Committee, Dr. Patrick Sullivan, Dr. Lance Johnson, and Dr. Sara Police. Each individual provided insights and support that guided and challenged my thinking, substantially improving the finished product.

In addition to the technical and instrumental assistance above, I received equally important assistance from family and friends. My parents, Joseph and Susan Yackzan, inspired me to take on this challenge, provided me with on-going support throughout the thesis process, and offered technical assistance critical for completing the project in a timely manner.

## Table of Contents

ACKNOWLEDGMENTS.....	iii
TABLE OF CONTENTS.....	iv
LIST OF TABLES.....	vi
LIST OF FIGURES.....	vii
1. INTRODUCTION.....	1
2. MATERIALS AND METHODS.....	3
2.1.    EXPERIMENTAL DESIGN.....	3
2.2.    FECAL SAMPLE COLLECTION.....	4
2.3.    GUT MICROBIOME ANALYSIS.....	5
2.4.    DIVERSITY AND DISSIMILARITY ANALYSIS.....	5
2.5.    METABOLOMIC PROFILING.....	5
2.6.    SHORT CHAIN FATTY ACID ANALYSIS OF PLASMA AND CECAL CONTENTS.....	6
2.7.    BLOOD GLUCOSE AND KETONE BODIES MEASUREMENTS.....	6
2.8.    CEREBRAL BLOOD FLOW (CBF) AND DIFFUSION TENSOR MRI (DT-MRI OR DTI) SCANS.....	6
2.9.    STATISTICAL ANALYSIS.....	7
3. RESULTS.....	8
3.1.    DIET AND APOE GENOTYPE EFFECTS.....	8
3.1.1. <i>Mice fed the ketogenic diet (KD) maintained a lower body weight despite increased caloric intake throughout the study.</i> .....	8
3.1.2. <i>Ketogenic diet disparately modulated blood ketone bodies (KBs) and glucose levels.</i> .....	9
3.1.3. <i>The KD induced recovery in E4 metabolic profile.</i> .....	10
3.1.4. <i>KD enhanced E4 metabolic profile compared to controls.</i> .....	11
3.1.5. <i>KD modulates brain physiology (vasculature and white matter myelination).</i> .....	15
3.1.6. <i>KD increased beneficial SCFA levels in plasma of KD mice.</i> .....	16
3.1.7. <i>APOE genotype more strongly influenced alpha diversity within the gut microbiome than diet.</i> .....	19
3.1.8. <i>APOE genotype mediated KD alterations to gut microbial profile.</i> .....	19
3.1.9. <i>KD enhanced microbiome composition by promoting Firmicutes proliferation and impeding Bacteroidetes growth.</i> .....	20
3.1.10. <i>KD cultivated similar microbial colonies within the gut of E3 and E4 mice compared to bacterial colonies within mice fed control diet.</i> .....	21
3.2.    SEX EFFECTS.....	23



3.2.1. <i>KD reduced weight gain in all groups relative to controls, excepting the APOE3 females.</i>	23
3.2.2. <i>Diet and genotype both strongly modulated blood ketone body concentration, while diet and sex both strongly influenced blood glucose concentrations.</i>	23
3.2.3. <i>KD intervention induced remarkable metabolic function recovery in E4 females compared to controls.</i>	24
3.2.4. <i>Genotype effects modulated DTI measurements more than sex or diet. Diet effects influenced CBF in the hippocampus and thalamus.</i>	26
3.2.5. <i>Sex and diet heavily modified SCFA production and transport.</i>	28
3.2.6. <i>Sex disparately altered gut microbial species diversity in E4 male and female mice.</i>	30
3.2.7. <i>Sex contributed to differences between gut microbial profiles in both E3 and E4 mice.</i>	31
4. DISCUSSION	33
APPENDIX	38
REFERENCES	50
VITA	54

## List of Tables

Table 1. Detailed breakdown of the final $n$ for each of the 8 study groups.....	4
Table 2. Comparison of special diet compositions.....	4
Table 3. Ketogenic diet (KD) intervention reduces weight gain in APOE3 and APOE4 mice.....	9
Table 4. KD effects on cortical metabolite concentrations.....	12-14
Table 5. KD reduces weight gain for all groups except APOE3 females.....	23
Table 6. KD effects on cortical metabolite concentrations.....	25
Table 7. Results summary table. ....	33
Table 8: Description of Metabolon QC samples .....	39
Table 9: Metabolon QC standards.....	39
Table 10: Example of q-value interpretation.....	49

## List of Figures

Figure 1. Study design.....	3
Figure 2. KD effects on blood glucose and ketone body levels. ....	10
Figure 3. KD and APOE genotype modulate DTI and CBF measures.....	16
Figure 4. KD and APOE genotype effects on plasma and cecum SCFA levels.....	18
Figure 5. KD and APOE genotype effects on alpha- and beta-diversity.....	19
Figure 6. KD effects on relative abundance of microbial phyla <i>Firmicutes</i> , <i>Bacteroidetes</i> , and <i>Proteobacteria</i> . ....	21
Figure 7. KD effects on microbial profile similarity. ....	22
Figure 8. KD, APOE genotype, and sex effects on blood glucose and ketone body levels. ....	24
Figure 9. Sex effects in DTI and CBF measures. ....	27
Figure 10. Sex effects on plasma and cecum SCFA levels. ....	29
Figure 11. Sex effects on alpha- and beta-diversity. ....	31
Figure 12. Sex effects on microbial gut composition.....	31-32
Figure 13. Preparation of client-specific technical replicates.....	40
Figure 14: Visualization of data normalization steps for a multiday platform run.....	43

## 1. INTRODUCTION

Alzheimer's disease (AD) is a progressive neurodegenerative disorder characterized by a decline in cognitive function and the development of dementia. AD is currently the most common global cause of dementia and prevalence continues to rise with few available treatments of only limited efficacy (Lane et al., 2018). The apolipoprotein  $\epsilon 4$  (APOE4) allele is the single greatest genetic risk factor for sporadic (late-onset) AD: E4 homozygotes have an eight- to twelve-fold increased risk compared E3 homozygotes (2021). In addition to genetics, a marked sex difference in response to the APOE4 allele has also been demonstrated in humans: female E4 carriers have a greater risk of developing AD, show accelerated progression of the disease, and have more severe cognitive and memory decline than males with the same APOE polymorphism (Altmann et al., 2014).

Although AD is a neurodegenerative disorder, accumulating evidence suggests that systemic metabolic dysfunction and inflammation contribute greatly to the risk of developing AD. Recent research highlights the presence of neurometabolic and neurovascular deficits decades before clinical presentation in APOE4 carriers. In line with this, patients with AD show metabolic dysfunction, such as impaired glucose utilization in the brain (Calsolaro and Edison, 2016). Impaired glucose metabolism can subsequently contribute to the development of insulin resistance, Type II diabetes mellitus (T2DM), hyperlipidemia, obesity, or other metabolic disorders that may further increase the risk of AD (Pistollato et al., 2016). Short-Chain Fatty Acid (SCFA) deficiency has been associated with T2DM; metabolic dysfunction including inflammation, insulin resistance and endoplasmic reticulum stress, are known to underlie T2DM in peripheral tissues (Hotamisligil, 2006). A similar condition has also been described in the brains of AD patients; thus, some groups have even described AD as Type 3 diabetes mellitus (T3DM) (Nguyen et al., 2020). Interventions that could alleviate inflammation and restore metabolic function systemically may ultimately reduce the risk of T2DM and AD. Another risk factor related to metabolic syndrome is dysbiosis of the gut microbiota, which is also considered to contribute to AD development through unknown mechanisms (Altmann et al., 2014; Pistollato et al., 2016).

Cerebral blood flow (CBF) reductions also occur in AD, and the E4 allele contributes to CBF reductions in pre-symptomatic E4-carriers prior to any decline in cognitive function (Matsuda, 2001). This hypoperfusion is thought to be yet another contributing factor to AD pathogenesis due to an inability for the body to appropriately supply necessary metabolites to the brain in concert with diminished clearance of A-Beta plaques accumulating in the brain's vasculature. In addition to changes in cerebral perfusion, diffusion tensor MRI (DT-MRI or DTI) measurements in AD patients have shown a decline in white matter integrity in AD brains (Bozzali et al., 2002). Whether or not there is evidence of similar changes in pre-clinical AD E4-carriers is currently up for debate. This decline in white matter integrity is thought to be a byproduct of cerebral hypometabolism, leading to a compensatory response that scavenges the brain for energy sources and ultimately strips away myelin sheaths to repurpose as fatty acid energy metabolites.

In response to the growing evidence of gut microbiota and metabolic deficiencies, dietary interventions are now being explored as a possible treatment for AD. Recent studies demonstrating that treatment of systemic inflammation and metabolic dysfunction can reverse cognitive decline and prevent development of AD (Bredesen et al., 2016). These studies encourage us to anticipate that early KD intervention can reduce the risk of developing AD.

The ketogenic diet (KD) is a low-carbohydrate and fat-rich diet that has been used in treating epilepsy (Baranano and Hartman, 2008), Parkinson's disease (Wlodarek, 2019), amyotrophic lateral sclerosis (Zhoa et al., 2006), and autism (Napoli et al., 2014). Attention has turned to KD as a possible clinical intervention because it induces a metabolic state of ketosis in which the brain and body uses ketone bodies (KBs) as an adaptive fuel source to supplement the insufficient carbohydrate energy supply (Cunnane et al., 2016; Rusek et al., 2019). Furthermore, KBs are considered a more efficient energy source than glucose, as they bypass glycolysis and directly enter the Krebs Cycle. KBs have also been associated with neuroprotective properties (Maalouf et al., 2009). These properties of KBs have the potential to alleviate the effects of the impaired glucose metabolism associated with AD. Moreover, the diet may help to reduce the accumulation of A $\beta$  plaques and reverse A $\beta$  toxicity (Broom et al., 2019). Research has also shown that

KD modulates both gut microbiome and SCFA levels in AD patients (Ma et al., 2018; Nagpal et al., 2019). Research in wildtype mice demonstrates that KD can improve CBF as well (Ma et al., 2018).

Despite the growing interest in KD, there is a lack of research into the interactions between sex, genotype, and diet. Therefore, the purpose of this study was to investigate KD as a nutritional intervention for AD prevention in young APOE3 and APOE4 male and female transgenic mouse models of AD. We fed (9 week) old mice either a ketogenic or control diet for (16) weeks. In this study, we investigated the effects of KD on body weight, blood ketone bodies and glucose levels, brain metabolites, short chain fatty acid levels in cecum and plasma, and gut microbiome diversity and composition.

## 2. MATERIALS AND METHODS

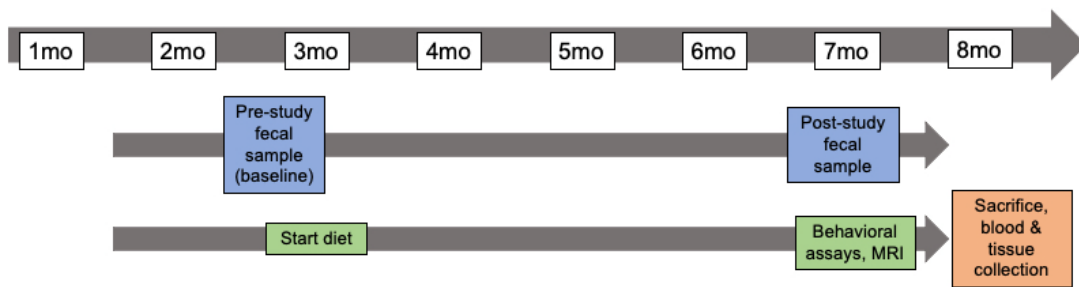


**Figure 1. Study design.** Special diet regimens were introduced at 12 weeks (3 months) of age. The study mice were fed special diet for 16 weeks (4 months). Pre-study fecal samples were collected before special diets were given. Post-study fecal samples were collected 16 weeks after diet start. Behavioral assessments and MRI scans were done after 16 weeks of feeding, then the study mice were sacrificed for blood and tissue collection.

### 2.1. Experimental design.

C57BL/6 transgenic human APOE3 and APOE4 male and female mice (6-9 weeks of age) were obtained from Taconic for use in this study (Model numbers 1548 and 1549, respectively). We determined the sample size with the power that could perform the comparison at a 0.05 level of significance, with a 90% chance of detecting a true

difference of all the measurements between the two groups;  $n = 6-12$  per group were used in the study – **Table 1** shows a detailed breakdown for the  $n$  of each study group.

**Table 1.** Detailed breakdown of the final  $n$  for each of the 8 study groups.

<b>APOE Genotype</b>	<i>Male Control</i>	<i>Male KD</i>	<i>Female Control</i>	<i>Female KD</i>
<b>APOE3</b>	n = 11	n = 9	n = 12	n = 12
<b>APOE4</b>	n = 9	n = 9	n = 12	n = 6

After arriving at our facilities, each mouse was given its own cage housed in a specific pathogen-free facility to avoid microbiome transfer. Both the control diet regimen (type 1515) and ketogenic diet regimen (type F3666) were obtained from Bio-Serv (**Table 2**). Fecal samples were obtained at two timepoints (baseline and post-study), and all mice were fed ad libitum for 16 weeks, with the diet beginning at 12 weeks of age (Figure 1). Body weight was measured every two weeks. The amount of remaining diet was weighed every two weeks to determine the food intake of the mice. All experimental procedures were performed according to NIH guidelines and approved by the Institutional Animal Care and Use Committee (IACUC) at the University of Kentucky (UK).

**Table 2.** Comparison of composition of caloric content between the special Control diet and Ketogenic diet (KD).

	<b>Control Diet Caloric Profile</b>		<b>Ketogenic Diet Caloric Profile</b>	
	<b>kcal/g</b>	<b>percent</b>	<b>kcal/g</b>	<b>percent</b>
Carbohydrate	2.61	69%	0.13	2%
Fat	0.46	12%	6.76	93%
Protein	0.72	19%	0.34	5%
<b>Total</b>	<b>3.79</b>	<b>100%</b>	<b>7.24</b>	<b>100%</b>

## 2.2. Fecal Sample Collection.

Fecal samples were collected by putting each mouse in a clean autoclaved cage and waiting for it to defecate normally. Samples were collected during a 2-hour window from

8 a.m. to 10 a.m. and frozen at  $-80^{\circ}\text{C}$  until further use. Samples were used to obtain genomic DNA. QIAGEN DNeasy PowerSoil Kit was used per manufacturers' guidelines.

### **2.3. Gut Microbiome Analysis.**

Shotgun metagenomic sequencing was done by CosmosID. Briefly, DNA libraries were assembled using the CosmosID proprietary library prep kit and pooled by adding an equimolar ratio of each sample on a high sensitivity chip to estimate size. Libraries were then sequenced using an Illumina NextSeq/HiSeq platform. Unassembled reads were directly analyzed by the CosmosID bioinformatics platform (CosmosID Inc., Rockville, MD), which allows for multi-kingdom microbiome analysis, profiling of antibiotic resistance and virulence genes, and quantification of relative abundance. CosmosID uses a high-performance k-mer based algorithm that disambiguates hundreds of millions of short reads of a sample into the microorganisms that the sequences represent. Matrix tables of detected taxa were generated, and heat maps were produced. These allow for visualization of diversity and abundance of each microbial taxa. LEfSe differential abundance analyses were performed between pairs of cohorts to determine taxa that are significantly enriched in each cohort.

### **2.4. Diversity and Dissimilarity Analysis.**

Alpha diversity (within sample, Shannon index) and beta diversity (dissimilarities between samples, Bray-Curtis index) were performed in order to compare the microbial community as a whole between different sample groups (i.e. diet, injury). Alpha and beta diversity analyses were performed by CosmosID (Rockville, MD). Visualizations of alpha diversity were created using GraphPad Prism 9.0. Visualizations of beta diversity were created by CosmosID (Rockville, MD), with corresponding PERMANOVA tests, respectively.

### **2.5. Metabolomic Profiling.**

All mice were euthanized following MRI scanning with subsequent collection of the right and left hemispheres of the brain. The tissues were separated into individual tubes and stored at  $-80^{\circ}\text{C}$ . The right hemisphere of each mouse brain was shipped on dry ice to Metabolon Inc. (Durham, NC, USA) for subsequent targeted and nontargeted



metabolomics analysis. The nontargeted metabolomics protocol has been described previously in (Hoffman et al., 2019). The targeted metabolomics protocol has been described in (Evans et al., 2009). See Appendix A for the full protocol from Metabolon Inc.

## **2.6. Short Chain Fatty Acid Analysis of Plasma and Cecal Contents.**

Eight SCFAs from cecum and plasma were analyzed with LC-MS/MS by Metabolon Inc. (Morrisville, NC): acetic acid (C2), propionic acid (C3), isobutyric acid (C4), 2-methylbutyric acid (C5), isovaleric acid (C5), valeric acid (C5), and caproic acid (C6). Both sets of samples were stable labeled with internal standards and homogenized in an organic solvent. The samples were then centrifuged followed by an aliquot of the supernatant used to derivatize to form SCFA hydrazides. This reaction mixture was subsequently diluted, and an aliquot was injected into an Agilent 1290/AB Sciex QTrap 5500 LCMS/MS system.

## **2.7. Blood Glucose and Ketone Bodies Measurements.**

Blood samples were collected during sacrifice in 500 µl EDTA blood collection tubes (Vacutainer K2 EDTA) to avoid blood coagulation. A total of 1–2 µl of blood sample were used to measure blood glucose level using a blood glucose meter and a test strip (Clarity Plus, Boca Raton, FL, USA). Another 10 µl of blood sample was used for ketone bodies level measurement using a STAT-Site M (β-Hydroxybutyrate) meter and a test strip (Standbio Ketosite STAT-Site M-β HB, Boerne, TX, USA).

## **2.8. Cerebral Blood Flow (CBF) and Diffusion Tensor MRI (DT-MRI or DTI) scans.**

We used the 7T Clinscan MR scanner (Siemens, Germany) at the Magnetic Resonance Imaging & Spectroscopy Center of UK. Mice were anesthetized with 4.0% isoflurane for induction and then maintained in a 1.2% isoflurane and air mixture using a facemask. Heart rate (90–130 bpm.), respiration rate (70-90 breaths per minute), and rectal temperature ( $37 \pm 0.5^\circ\text{C}$ ) were monitored. A water bath with circulating water at 45–50°C was used to maintain the body temperature. Quantitative CBF (with units of mL/g per minute) was measured using MRI-based pseudo-continuous arterial spin

labeling (pCASL) techniques (Muir et al., 2008). Paired images were acquired in an interleaved fashion with FOV = 18 x 13.5 mm<sup>2</sup>, matrix = 64 x 48, slice thickness = 1 mm, 6 slices, labeling duration = 200ms, TR = 4,000 ms, TE = 20 ms, and 120 repetitions. pCASL image analysis was employed with in-house written codes in MATLAB (MathWorks, Natick, MA) to obtain quantitative CBF (Lin et al., 2015). CBF maps were visualized and quantitated using Mango image viewer (UT San Antonio, TX). Diffusion tensor imaging (DTI) is used to characterize microstructural changes in the brain (Alexander et al., 2007). The images are acquired using four-segment, spin-echo, echo-planar sequence with the following parameters: field of view = 22 x 14.3 mm, 160 x 160 matrix, slice thickness = 1 mm, slice numbers = 4, TR = 1400 ms, TE = 42 ms, 90 degree flip angle, *b* value = 0 and 800 s/mm<sup>2</sup>, diffusion direction = 106, diffusion gradient amplitude (G) = 10 and 190 mT/m, gradient duration ( $\Delta$ ) = 18 ms, and averages = 1 (Guo et al., 2015). Fractional Anisotropy (FA) values are analyzed using Mango image viewer for regions of interest.

## **2.9. Statistical analysis.**

All statistical analyses were completed using GraphPad Prism (GraphPad, San Diego, CA, USA). 2-way ANOVA tests were performed for determination of differences between diet and genotype groups followed by Tukey's multiple comparisons test. 3-way ANOVA tests were performed for determination of differences between sexes followed by Tukey's multiple comparisons test. Levels of statistical significance were reached when  $p < 0.05$ . Data are represented as mean  $\pm$  S.E.M. For both the metabolite and microbiome analysis, given the multiple comparisons inherent in analysis of metabolites, between-group relative differences are assessed using both p-value and false discovery rate analysis (q-value).

### 3. RESULTS

#### 3.1. Diet and APOE Genotype Effects

##### 3.1.1. Mice fed the ketogenic diet (KD) maintained a lower body weight despite increased caloric intake throughout the study.

As mentioned in the Introduction, AD risk is subject to both genetic and non-genetic factors. Weight and dietary habits is one such risk factor that can contribute to AD. Similar to previous studies in APOE-TR mice(Lane-Donovan and Herz, 2016), we found significant diet effects on body weight for both APOE genotypes (**Table 3**). Post-hoc analysis showed significant weight loss in KD groups relative to respective Control groups (for APOE3 and APOE4:  $p = 0.0079$ ).

We observed significant diet effects on caloric consumption for comparisons within the E3 and E4 groups (data not shown). Post-hoc analysis revealed significantly increased caloric consumption for E3-KD over E3-Ctrl during Week 5 ( $p = 0.0128$ ), Week 9 ( $p = 0.0016$ ), Week 11 ( $p < 0.0001$ ), Week 13 ( $p = 0.0016$ ), and Week 15 ( $p = 0.0244$ ). Additionally, post-hoc analysis showed significantly increased caloric consumption for E4-KD over E4-Ctrl in Week 5 ( $p = 0.0006$ ), Week 11 ( $p = 0.0006$ ), and Week 15 ( $p = 0.0011$ ).

We also noted significant APOE genotype effects on caloric consumption between the Control and KD groups. Post-hoc analysis showed significantly increased caloric consumption for E3-KD over E4-KD during Week 7 ( $p = 0.0083$ ), Week 9 ( $p = 0.0043$ ), and Week 13 ( $p = 0.0464$ ). We found no significant differences in caloric consumption for comparisons between E3- and E4-Ctrl groups.

**Table 3. Ketogenic Diet (KD) intervention reduces weight gain in APOE3 and APOE4 mice.** A two-way ANOVA showed significant diet effects ( $F(1,76) = 10.89$ ;  $p = 0.0015$ ), but no significant genotype effects. Post-hoc analysis showed significant weight gain in Control Diet groups compared to respective KD groups (for APOE3 and APOE4:  $p = 0.0079$ ).

<i>APOE Genotype</i>	<b>APOE3</b>	<b>APOE4</b>
<i>Control Diet (g)</i>	35.39 ± 4.32	36.56 ± 5.63
<i>Ketogenic Diet (g)</i>	32.88 ± 5.36	31.23 ± 4.73

### 3.1.2. Ketogenic diet disparately modulated blood ketone bodies (KBs) and glucose levels.

It has been established that ketone body metabolism contributes neuroprotective benefits, improvements in mitochondrial efficiency, enhanced protection against reactive oxygen species (ROS), along with many other metabolic advantages. Consistent with previous KD studies in WT mice (Kennedy et al., 2007; Ma et al., 2018), we found significant diet effects on blood KBs for the E3 and E4 comparisons ( $F(1,63) = 40.49$ ,  $p < 0.0001$ ; **Fig. 2A**). Post-hoc analysis showed significantly elevated levels of blood KBs in E3-KD over E3-Ctrl ( $p < 0.0001$ ) and E4-KD over E4-Ctrl mice ( $p = 0.0015$ ). There were no significant APOE genotype effects on blood KB ( $F(1,63) = 0.3061$ ,  $p = 0.5820$ ). Diet effects were also present for blood glucose levels ( $F(1,49) = 5.35$ ,  $p = 0.0250$ ; **Fig. 2B**) with a tendency for lower glucose levels following KD. However, post-hoc analysis did not show statistical significance between groups for either E3 ( $p = 0.1004$ ) or E4 mice ( $p = 0.7882$ ). We did not find APOE genotype effects on blood glucose, either ( $F(1,49) = 3.23$ ,  $p = 0.0787$ ).

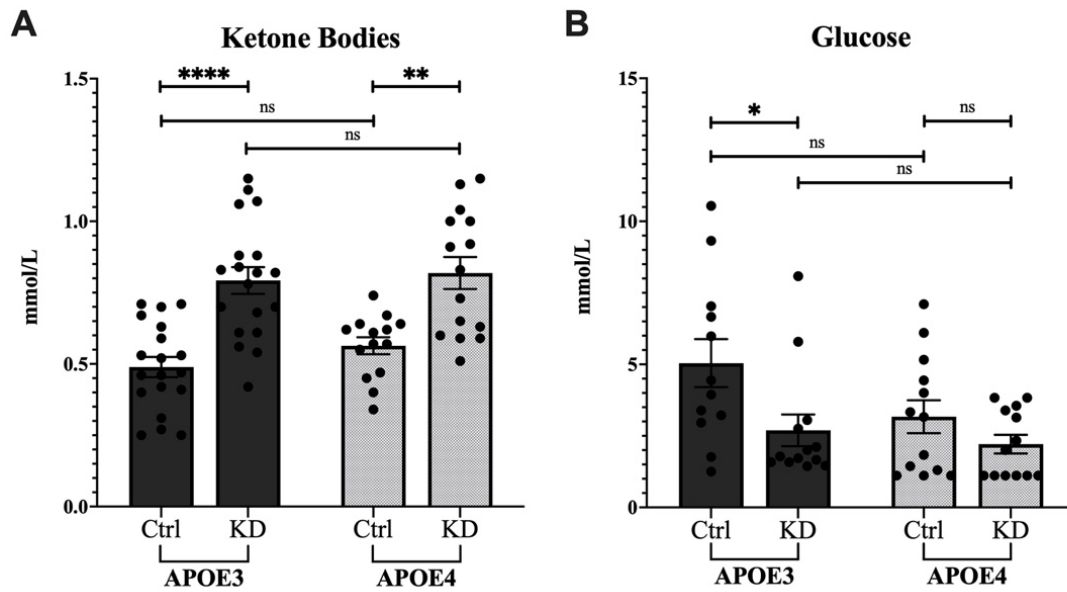


**Figure 2. KD effects on blood glucose and ketone body levels. (A)** Both APOE3-KD and APOE4-KD mice had significantly higher blood KB levels compared to their control counterparts. **(B)** KD mice trended towards lower blood glucose levels, but differences did not reach statistical significance in either APOE3 or APOE4 group. \* $p < 0.05$ ; \*\* $p < 0.01$ ; \*\*\*\* $p < 0.0001$ .

### 3.1.3. The KD induced recovery in E4 metabolic profile.

To determine the effects of genotype on general metabolic health, the right hemisphere of each mouse cortex was sent for metabolomic profiling. Genotype contrasts within control diet groups revealed E4-Ctrl had significantly reduced cortical concentrations of many amino acids and their neurotransmitter derivatives (aspartate, asparagine, glutamate, glutamine, and GABA), as well as most TCA cycle intermediates (citrate, aconitate, isocitrate, succinylcarnitine, succinate, fumarate, and malate) compared to E3-Ctrl (**Table 4A**). Additionally, E4-Ctrl had significantly higher cortical concentrations of oxidized glutathione, potentially highlighting a dysregulation in antioxidant mechanisms for E4 mice on Control diet. (**Table 4A**).

#### **3.1.4. KD enhanced E4 metabolic profile compared to controls.**

Diet group comparisons within the E4 groups revealed KD induced a significant increase in cortical concentrations of glutamate, glutamine, GABA, dopamine, serotonin, and malate (**Table 4B**), suggesting the KD did indeed counteract APOE4-associated metabolic deficits. Among the E3 mice, KD significantly reduced cortical levels of many carbohydrate metabolic intermediates (DHAP, PEP, lactate, UDP-glucose, and UDP-galactose), possibly indicative of a metabolic shift away from carbohydrates in the E3-KD mice (**Table 4B**). Interestingly, E3-KD mice had reduced levels of both reduced and oxidized glutathione, which could mean antioxidant dysfunction or simply higher mitochondrial efficiency and a reduced need for ROS mitigation.

**Table 4. KD effects on cortical metabolite concentrations. (A)** Genotype effects in Control groups show reduced metabolite levels in E4-Ctrl; KD comparisons showed recovery in TCA cycle metabolites for E4 mice. **(B)** KD enhanced both E3 and E4 metabolic profile compared to respective controls.

Table 4A				
Super Pathway	Sub Pathway	Biochemical Name	ANOVA Contrasts - Fold of Change	
			<u>E4</u> E3	
			Control	K e t o
Amino Acid	Alanine and Aspartate Metabolism	aspartate	0.79	0.91
		N-acetylaspartate (NAA)	1.10	1.17
		asparagine	0.80	0.91
	Glutamate Metabolism	glutamate	0.77	1.17
		glutamine	0.68	1.01
		N-acetyl-aspartyl-glutamate (NAAG)	0.86	0.97
		gamma-aminobutyrate (GABA)	0.63	0.94
	Glutathione Metabolism	glutathione, reduced (GSH)	0.87	1.76
		glutathione, oxidized (GSSG)	1.01	1.11
Carbohydrate	Glycolysis, Gluconeogenesis, and Pyruvate Metabolism	phosphoenolpyruvate (PEP)	0.89	1.19
		pyruvate	1.14	1.38
Energy	TCA Cycle	citrate	0.68	0.84
		aconitate [cis or trans]	0.64	0.80
		isocitrate	0.61	0.81
		succinylcarnitine (C4-DC)	0.78	1.27
		succinate	0.35	1.04
		fumarate	0.68	0.79
		malate	0.68	0.93

<b>Table 4A</b>				
Lipid	Fatty Acid Metabolism	acetyl CoA	<b>0.92</b>	<b>1.40</b>
	Long Chain Saturated Fatty Acid	palmitate (16:0)	<b>0.84</b>	<b>0.68</b>
		stearate (18:0)	<b>0.85</b>	<b>0.67</b>
		arachidate (20:0)	<b>0.84</b>	<b>0.69</b>
	Long Chain Polyunsaturated Fatty Acid (n3 and n6)	eicosapentaenoate (EPA; 20:5n3)	<b>0.92</b>	<b>0.49</b>
		linoleate (18:2n6)	<b>1.13</b>	<b>0.51</b>
		arachidonate (20:4n6)	<b>0.84</b>	<b>0.87</b>
	Carnitine Metabolism	carnitine	<b>0.89</b>	<b>1.03</b>
	Ketone Bodies	3-hydroxybutyrate (BHBA)	<b>1.01</b>	<b>0.70</b>
	Neurotransmitter	acetylcholine	<b>0.83</b>	<b>1.35</b>
	Phospholipid Metabolism	choline	<b>0.98</b>	<b>0.95</b>
		choline phosphate	<b>0.97</b>	<b>0.95</b>
		glycerophosphoethanolamine	<b>0.82</b>	<b>1.08</b>
	Glycerolipid Metabolism	glycerol	<b>0.83</b>	<b>0.96</b>
Sterol	cholesterol sulfate	<b>1.29</b>	<b>0.98</b>	



Table 4B				
Super Pathway	Sub Pathway	Biochemical Name	ANOVA Contrasts - Fold of Change	
			Keto Control	
			E3	E4
Amino Acid	Glycine, Serine and Threonine Metabolism	N-acetylglycine	1.46	1.62
	Glutamate Metabolism	glutamate	0.91	1.38
		glutamine	0.96	1.43
		gamma-aminobutyrate (GABA)	0.95	1.41
	Tyrosine Metabolism	tyrosine	1.21	1.07
		dopamine	0.85	1.63
	Tryptophan Metabolism	serotonin	0.79	1.21
	Methionine, Cysteine, SAM and Taurine Metabolism	hypotaurine	1.13	0.74
		taurine	0.85	0.91
	Urea cycle; Arginine and Proline Metabolism	urea	0.65	0.95
Glutathione Metabolism	glutathione, reduced (GSH)	0.57	1.14	
	glutathione, oxidized (GSSG)	0.82	0.90	
Carbohydrate	Glycolysis, Gluconeogenesis, and Pyruvate Metabolism	dihydroxyacetone phosphate (DHAP)	0.82	1.06
		phosphoenolpyruvate (PEP)	0.78	1.05
		lactate	0.86	0.98
	Nucleotide Sugar	UDP-glucose	0.66	0.98
		UDP-galactose	0.73	1.20
Energy	TCA Cycle	malate	0.93	1.27
		2-methylcitrate/homocitrate	1.35	1.22

### 3.1.5. KD modulates brain physiology (vasculature and white matter myelination).

DTI is emerging as a novel imaging technique for indexing neuronal changes in white matter during AD development. Using this MRI technique, it has been well established that white matter damage accumulates during AD (Bozzali et al., 2002), however, the impact of APOE4 on white matter is less well characterized. We noted significant genotype differences in corpus callosum (CC) fraction anisotropy (FA) measurements taken via DTI scans ( $F(1,68) = 10.80$ ;  $p = 0.0016$ ; **Fig. 3A**). Post-hoc analysis showed enhanced white matter integrity in E3-Ctrl over E4-Ctrl ( $p = 0.0085$ ) and E3-KD over E4-KD ( $p = 0.0085$ ), suggesting the APOE4 allele may disrupt white matter integrity in a region-specific manner. We observed significant diet effects in averaged External Capsule (EC) FA values ( $F(1,68) = 5.558$ ;  $p = 0.0213$ ; **Fig. 3B**). Post-hoc analysis did not reveal further significant comparisons between groups. Lastly, we noticed significant genotype effects present in averaged Fimbria FA values ( $F(1,68) = 9.179$ ;  $p = 0.0035$ ; **Fig. 3D**). Post-hoc analysis revealed enhanced E3-Ctrl ( $p = 0.0178$ ) and E3-KD ( $p = 0.0178$ ) white matter integrity when compared to respective E4 diet groups, again, indicating an APOE4-related disruption of white matter integrity.

Arterial Spin Labeling (ASL) is another MRI technique used to assess tissue perfusion, or CBF. Previous research in AD has revealed global CBF reductions of up to 20% in AD patients compared to nondemented controls (Roher et al., 2012). Studies investigating APOE4 effects on CBF report that changes in CBF are largely determinant on age, and that hypoperfusion is generally seen in elderly APOE4 carriers compared to age-matched noncarriers, though this reduction is not always observed in younger E4 carriers (Hogh et al., 2001; Tai et al., 2016). Lastly, the KD has been shown to increase rCBF in young, wildtype (WT) mice (Ma et al., 2018). Our results indicated a significant effect of diet on average CBF of the left and right hippocampi ( $F(1,57) = 4.654$ ;  $p = 0.0352$ ; **Fig. 3G**). However, post-hoc analysis showed no significant individual comparisons. We did not observe any significant differences in CBF for the whole brain, cortex, or thalamus, though there is a noticeable trend of lower rCBF for Control mice

relative to respective KD mice. These results are not unexpected – the mice in this study were young and aging is a very large factor in CBF changes.

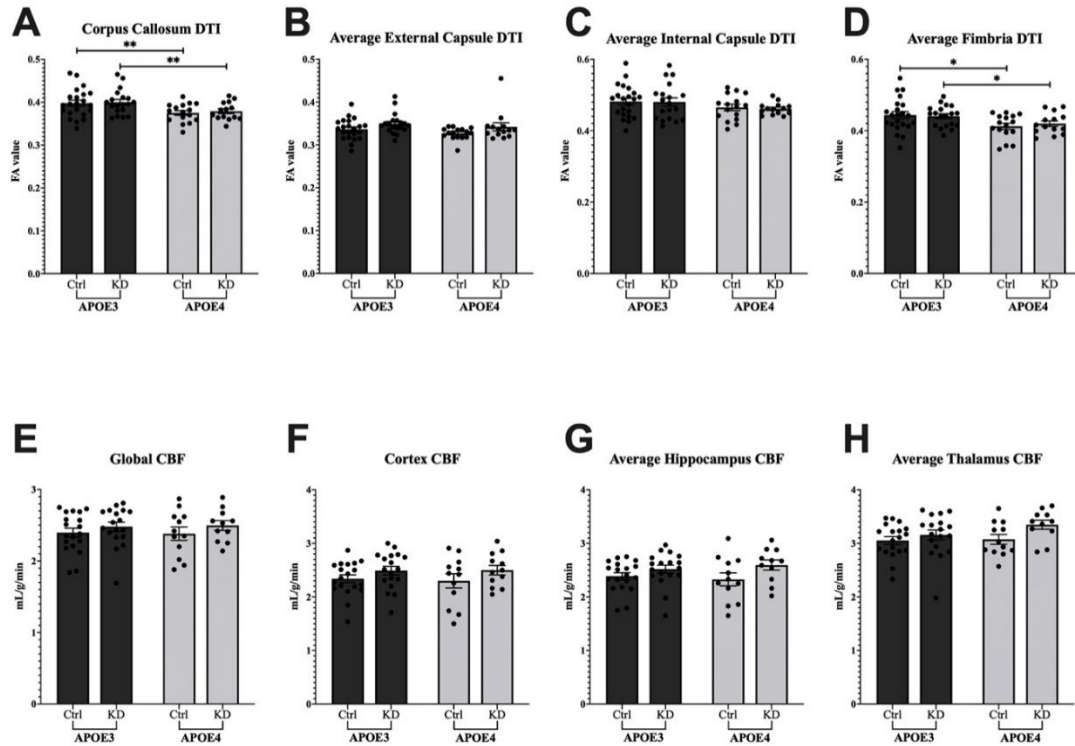


**Figure 3. KD and APOE genotype modulate DTI and CBF measures.** FA values for (A) corpus callosum, (B) averaged left and right external capsule, (C) averaged internal capsule, and (D) averaged fimbria. CBF values for (E) whole brain (global), (F) cortex, (G) averaged hippocampi, and (H) averaged thalamus. \*  $p < 0.05$ ; \*\*  $p < 0.01$ .

### 3.1.6. KD increased beneficial SCFA levels in plasma of KD mice.

Previous research points to a KD-induced increase in SCFA production mediated through changes in gut microbiota composition (Ma et al., 2018; Paoli et al., 2019). SCFAs possess neuroactive properties, such as enhancing blood-brain barrier (BBB) integrity, functioning as an alternative cellular energy source, increasing neurotransmitter reserves, modulating gene expression, and improving memory consolidation (Morrison and Preston, 2016; Silva et al., 2020). In addition to CNS benefits, SCFAs also provide an alternative fuel source to enterocytes, hepatocytes, and other peripheral tissues, influence cellular signaling and gene expression, and have even been shown to regulate

appetite, sleep, and immune system function (Morrison and Preston, 2016; Silva et al., 2020). We observed markedly significant diet effects on plasma acetic acid concentrations ( $F(1,54) = 158.8$ ;  $p < 0.0001$ ; **Fig. 4A**). Post-hoc analysis showed significantly elevated plasma acetic acid levels in both E3-KD ( $p < 0.0001$ ) and E4-KD ( $p < 0.0001$ ) compared to respective controls. Conversely, we observed a nonsignificant diet effect resulting in reduced acetic acid production in the cecum of E3-KD and E4-KD mice compared respective controls ( $F(1,55) = 0.7349$ ;  $p = 0.3950$ ; **Fig. 4B**).

We observed significant APOE genotype effects on plasma butyric acid concentrations ( $F(1,50) = 4.404$ ;  $p = 0.0409$ ; **Fig. 4C**). However, post-hoc analysis showed no significant comparisons existed between the different genotypes. Contrarily, we found significant diet effects on butyric acid production within the cecum ( $F(1,56) = 4.430$ ;  $p = 0.0398$ ; **Fig. 4D**). Post-hoc analysis showed no significantly different comparisons between groups for this measure.

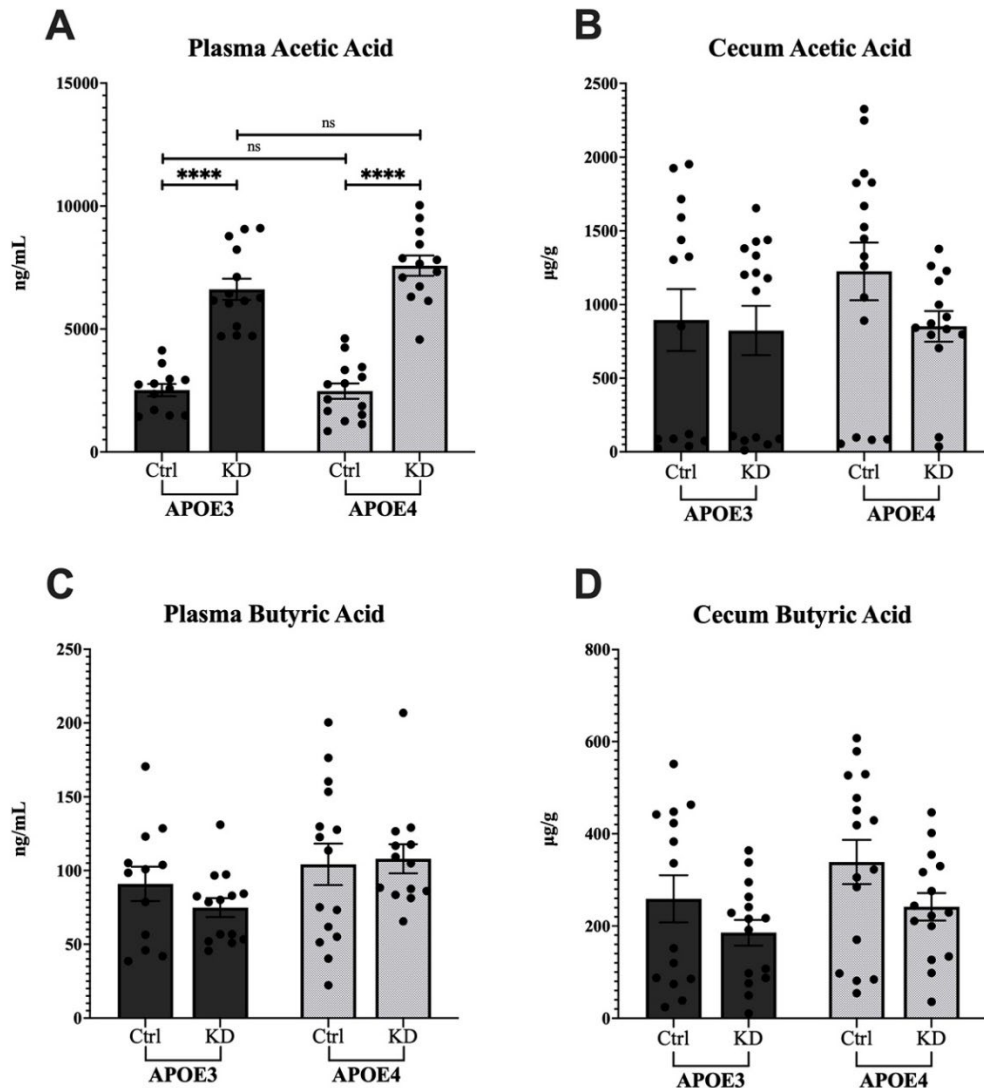


**Figure 4. KD and APOE genotype effects on plasma and cecum SCFA levels.**

(A) KD significantly increased E3-KD and E4-KD plasma levels of acetic acid compared to respective controls. (B) KD slightly reduced E3-KD and E4-KD acetic acid production in cecum compared to respective controls. (C) APOE genotype had significant influence on plasma butyric acid levels for E3-KD and E4-KD comparison, although no individual comparisons were noted. (D) KD significantly reduced butyric acid production in cecum, though no significant comparisons were detected.

### 3.1.7. APOE genotype more strongly influenced alpha diversity within the gut microbiome than diet.

As mentioned above, the APOE4 allele produces alterations in gut microbiome composition and diversity, leading to sustained gut dysbiosis. This chronic dysbiosis is thought to contribute to the pathogenesis of Alzheimer's disease through disrupting BBB integrity, impairing A $\beta$  clearance and CBF, and increased systemic and cerebral inflammation (Bostanciklioglu, 2019; Tran et al., 2019; Zajac et al., 2022). In line with this, we identified significant APOE genotype effects in alpha diversity (Shannon index) within the gut microbiome of E3 and E4 mice ( $F(1,53) = 6.992$ ;  $p = 0.0107$ ; **Fig. 5A**). However, post-hoc analysis did not identify any significant comparisons between the groups. Previous studies have shown the KD increases alpha diversity in WT mice (Ma et al., 2018), though our results do not show any significant effects of diet on alpha diversity.

### 3.1.8. APOE genotype mediated KD alterations to gut microbial profile.

Similar to a previous study (Ma et al., 2018), we observed significant diet effects on beta diversity in both the E3 and E4 comparisons, though the strength of the diet effects seems to be modulated based on genotype (Bray-Curtis index; **Fig. 5B, 5C**). KD engendered significant dissimilarity between E3-KD and E3-Ctrl gut microbial profiles ( $F(1,53) = 6.852$ ;  $p = 0.001$ ; **Fig. 5B**) and the E4-KD and E4-Ctrl gut microbial profiles ( $F(1,53) = 2.949$ ;  $p = 0.011$ ; **Fig. 5C**).

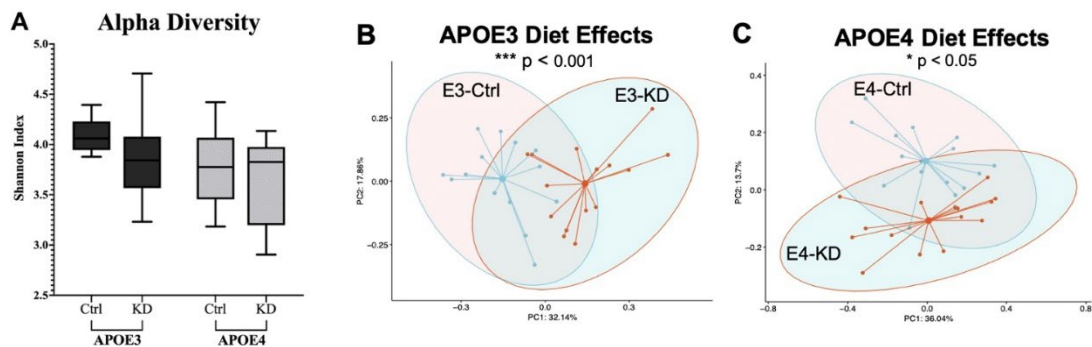


**Figure 5. KD and APOE genotype effects on alpha- and beta-diversity. (A)** KD reduced alpha diversity in E3-KD compared to E3-Ctrl, and in E4-Ctrl

compared to E3-Ctrl. KD significantly altered beta diversity in both **(B)** APOE3 and **(C)** APOE4 mice. \*  $p < 0.05$ ; \*\*  $p < 0.01$ ; \*\*\*  $p < 0.001$ .

### **3.1.9. KD enhanced microbiome composition by promoting *Firmicutes* proliferation and impeding *Bacteroidetes* growth.**

KD alterations in gut microbial composition have not been well characterized. To further analyze KD effects on the gut microbiome, we investigated the concentrations of phyla *Firmicutes*, *Bacteroidetes*, and *Proteobacteria*. We found that diet significantly affected the *Firmicutes*:*Bacteroidetes* (F:B) phyla ratio (F (1,50) = 7.585;  $p = 0.0082$ ; **Fig. 6A**). Post-hoc analysis showed no significant differences among group comparisons. Additionally, we observed significant diet effects on relative abundance of microbiota comprising phyla *Firmicutes* (F (1,56) = 7.233;  $p = 0.0094$ ; **Fig. 6B**). Once more, post-hoc analysis showed no significant differences among group comparisons. Lastly, we observed significant diet effects on relative abundance of microbiota belonging to phyla *Bacteroidetes* (F (1,56) = 15.58;  $p = 0.0002$ ; **Fig. 6C**). Post-hoc analysis revealed significantly decreased relative abundance of *Bacteroidetes* in E3-KD microbial profile compared to E3-Ctrl ( $p = 0.0080$ ).

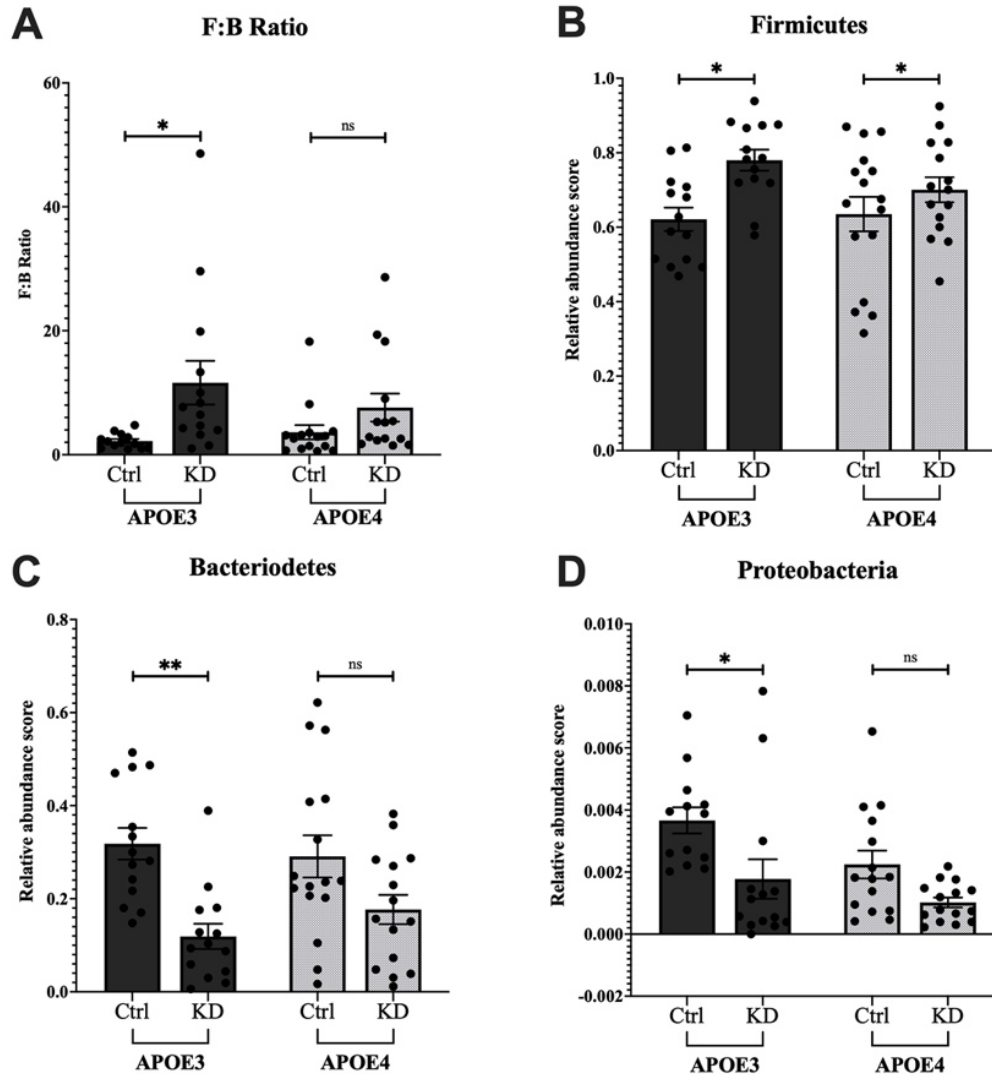


**Figure 6. KD effects on relative abundance of microbial phyla *Firmicutes*, *Bacteroidetes*, and *Proteobacteria*.** (A) KD affected the F:B ratio in E3 and E4 comparisons. (B) KD influenced *Firmicutes* relative abundance within the gastrointestinal tract. (C) KD influenced *Bacteroidetes* relative abundance within the gastrointestinal tract. (D) KD reduced *Proteobacteria* relative abundance within the gastrointestinal tract. \* P < 0.05; \*\* p < 0.01.

### 3.1.10. KD cultivated similar microbial colonies within the gut of E3 and E4 mice compared to bacterial colonies within mice fed control diet.

A LefSe analysis allows us to examine any significant changes in relative abundances among bacterial species due to KD intervention. The analysis revealed significantly



higher relative abundance of *Lactobacillus johnsonii* and *L. reuteri* within both E3-KD and E4-KD relative to respective controls. We also observed that Ctrl mice microbiome composition matched each other far more closely than KD mice microbial communities did. However, the few species in common among the KD mice are associated with beneficial health effects.

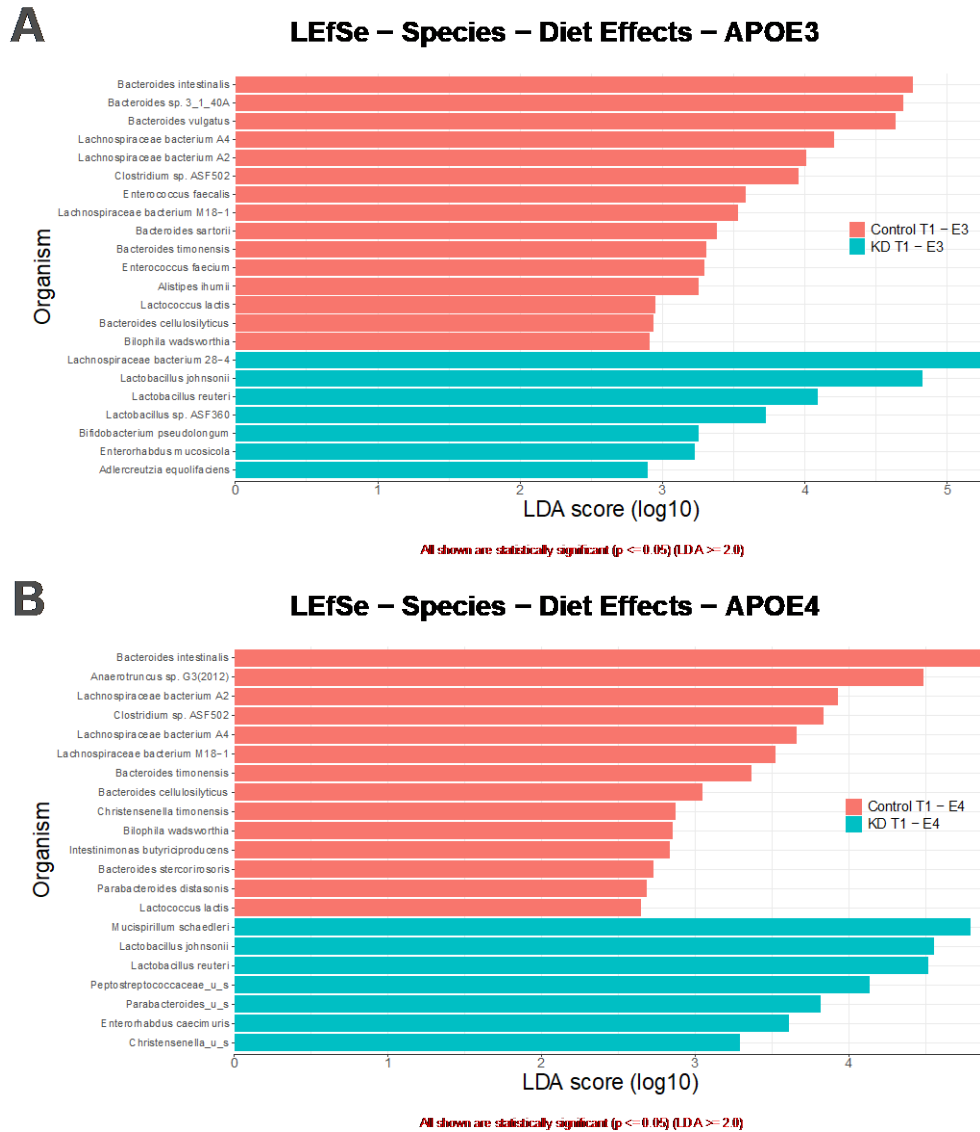


**Figure 7. KD effects on microbial profile similarity.** The LEfSe figure illustrates species of significantly different relative abundance between (A) E3-Ctrl and E3-KD and (B) E4-Ctrl and E4-KD.

### 3.2. Sex Effects

#### 3.2.1. KD reduced weight gain in all groups relative to controls, excepting the APOE3 females.

We observed significant diet effects for body weight measurements, but no genotype or sex effects. (**Table 5**). Post-hoc analysis revealed the E4-Ctrl males had significantly body weight gain than the E4-KD males ( $p = 0.0011$ ).

We also discovered diet and sex effects present for caloric consumption over week 6 ( $F(1,53) = 16.52$ ;  $p = 0.0002$ ), week 10 ( $F(1,51) = 36.01$ ;  $p < 0.0001$ ), week 14 ( $F(1,48) = 29.36$ ;  $p < 0.0001$ ), and week 16 ( $F(1,52) = 12.07$ ;  $p = 0.0010$ ; data not shown).

**Table 5. KD reduces weight gain for all groups except APOE3 Females.** A three-way ANOVA showed significant diet effects ( $F(1,71) = 13.88$ ;  $p = 0.0004$ ), but no significant effects on genotype or sex. Post-hoc analysis revealed significantly reduced weight for E4-KD mice relative to E4-Ctrl ( $p = 0.0011$ ).

<i>Genotype</i>	<b>APOE3 Male</b>	<b>APOE3 Female</b>	<b>APOE4 Male</b>	<b>APOE4 Female</b>
<i>Control Diet</i>	38.13 ± 2.48	32.88 ± 4.16	39.56 ± 2.75	34.30 ± 6.26
<i>Ketogenic Diet</i>	32.86 ± 4.12	32.89 ± 6.41	30.30 ± 4.12	32.62 ± 5.62

#### 3.2.2. Diet and genotype both strongly modulated blood ketone body concentration, while diet and sex both strongly influenced blood glucose concentrations.

We noted no significant sex effects present in ketone body concentration, though we detected very strong diet effects ( $F(1,51) = 41.40$ ;  $p < 0.0001$ ; **Fig. 8C**). However, post-hoc analysis revealed significantly increased ketone body levels in E4-KD males over E4-KD females ( $p = 0.0006$ ), showing the presence of sex effects in at least one comparison. Additionally, post-hoc analysis showed increased ketone body levels in both E3-KD males ( $p = 0.0017$ ) and E4-KD males ( $p = 0.0003$ ) when compared to respective male control counterparts; there were no significant differences between female E3-KD vs. E3-Ctrl or female E4-KD vs E4-Ctrl. Lastly, post-hoc analysis indicated significantly

increased ketone body levels in E3-KD females compared to E4-KD females ( $p = 0.0152$ ).

We recorded significant diet effects ( $F(1,44) = 5.249$ ;  $p = 0.0268$ ) and markedly significant sex effects ( $F(1,44) = 19.83$ ;  $p < 0.0001$ ; **Fig. 8D**) in blood glucose levels. Post-hoc analysis did not reveal any significant differences upon further group comparisons.

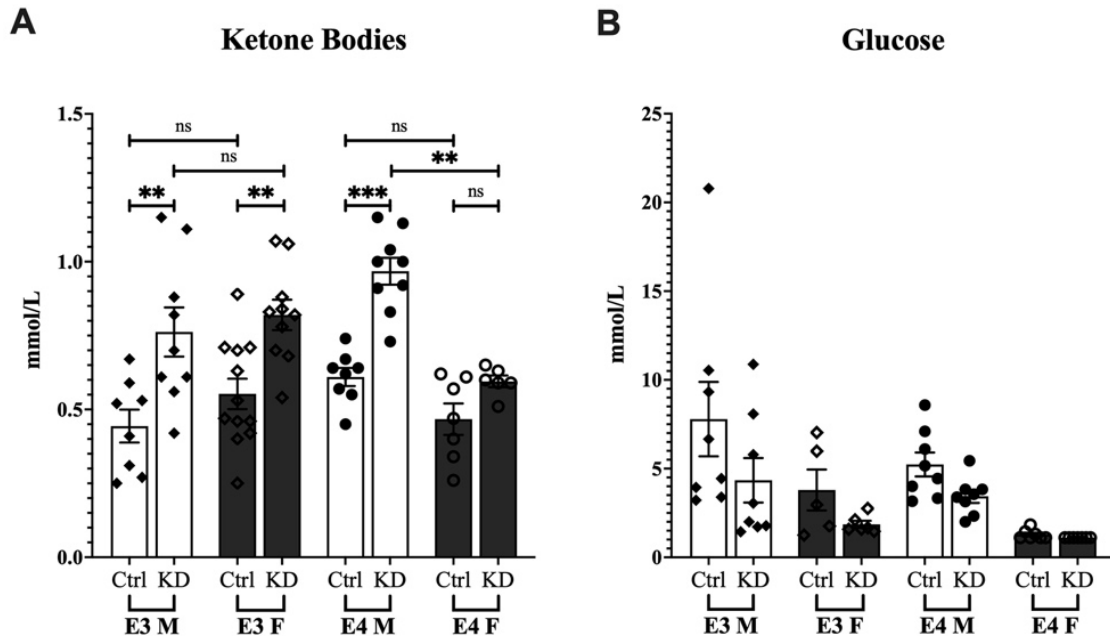


**Figure 8. KD, APOE genotype, and sex effects on blood glucose and ketone body levels. (A) Sex, diet, and genotype influence blood ketone body levels. (B) Sex and diet effects modulated blood glucose levels.**

### 3.2.3. KD intervention induced remarkable metabolic function recovery in E4 females compared to controls.

We observed massive KD-induced recovery in levels of crucial metabolites within cortical tissues of E4-KD females compared to E4-Ctrl females (**Table 6**). Metabolites that were significantly elevated in E4-KD females include NAA, multiple neurotransmitters (glutamate, glutamine, GABA, dopamine, and serotonin), along with

many TCA cycle intermediates (citrate, aconitate, isocitrate, alpha-ketoglutarate, succinylcarnitine, succinate, and malate). This KD enhancement was not seen among E4 males, E3 females and E3 males (**Table 6**).

We also compared metabolic profiles of E4-Ctrl females to E3-Ctrl females to determine baseline metabolic function between females of different genotypes (**Table 6**). This comparison revealed the E4 mice had significantly lower levels of almost all metabolites mentioned earlier (glutamate, glutamine, GABA, citrate, aconitate, isocitrate, alpha-ketoglutarate, succinylcarnitine, succinate, and malate). The only metabolites that were not significantly reduced at baseline were dopamine and serotonin. Interestingly, we also found that NAA was significantly elevated in E4-Ctrl females compared to E3-Ctrl females, as it was in E4-KD females over E4-Ctrl females.

**Table 6. KD effects on cortical metabolite concentrations.** Sex effects were markedly prevalent in E4 female mice, revealing massive recovery of metabolic profile in E4-KD females compared to respective controls.

Super Pathway	Sub Pathway	Biochemical Name	F Ctrl E4/E3	M Ctrl E4/E3	E4 F Keto/Ctrl	E4 M Keto/Ctrl	E3 F Keto/Ctrl	E3 M Keto/Ctrl
Amino Acid	Alanine and Aspartate Metabolism	N-acetylaspartate (NAA)	1.36	0.98	1.19	1.01	0.96	1.01
	Glutamate Metabolism	glutamate	0.36	1.13	3.36	0.80	1.01	0.85
		glutamine	0.29	1.10	3.18	0.90	1.00	0.95
		gamma-aminobutyrate (GABA)	0.24	1.13	3.33	0.84	1.06	0.84
	Tyrosine Metabolism	dopamine	0.50	0.57	3.11	1.20	0.80	0.84
	Tryptophan Metabolism	serotonin	0.78	0.73	2.19	1.00	0.86	0.74
Carb.	Pentose Phosphate Pathway	ribose 1-phosphate	1.41	0.91	1.19	0.92	0.79	0.92
Energy	TCA Cycle	citrate	0.38	1.11	1.93	0.83	1.18	0.76
		aconitate [cis or trans]	0.38	1.01	1.83	0.83	1.17	0.73
		isocitrate	0.37	0.97	1.76	0.82	1.09	0.66
		alpha-ketoglutarate	0.50	1.33	3.18	0.65	1.45	1.01
		Succinylcarnitine (C4-DC)	0.35	1.11	3.37	0.56	0.74	0.70
		succinate	0.22	0.42	5.25	1.36	0.80	0.76
		malate	0.42	0.99	1.92	0.92	0.94	0.95

### 3.2.4. Genotype effects modulated DTI measurements more than sex or diet. Diet effects influenced CBF in the hippocampus and thalamus.

We noted significant genotype differences in corpus callosum (CC) fraction anisotropy (FA) measurements taken via DTI scans ( $F(1,63) = 8.626$ ;  $p = 0.0046$ ; **Fig. 9A**). did not reveal further significant comparisons between groups. We observed significant diet effects in averaged External Capsule (EC) FA values ( $F(1,63) = 5.705$ ;  $p = 0.0199$ ; **Fig. 9B**). Post-hoc analysis did not reveal further significant comparisons between groups. We noted significant genotype ( $F(1,63) = 5.335$ ;  $p = 0.0242$ ) and sex effects ( $F(1,63) = 4.564$ ;  $p = 0.0365$ ; **Fig. 9C**) for averaged internal capsule (IC) FA values. Post-hoc analysis revealed E3-KD male mice had enhanced white matter integrity over both E4-KD males ( $p = 0.0386$ ) and E3-KD females ( $p = 0.0029$ ). Lastly, we

noticed significant genotype effects present in averaged Fimbria FA values ( $F(1,63) = 10.37$ ;  $p = 0.0020$ ; **Fig. 9D**), though post-hoc analysis did not show further significant comparisons.

We observed significant diet effects in CBF of averaged left and right hippocampi ( $F(1,52) = 4.994$ ;  $p = 0.0298$ ; **Fig. 9G**). However, post-hoc analysis showed no significant individual comparisons. We also noted significant diet effects for averaged thalami CBF values ( $F(1,52) = 4.133$ ;  $p = 0.0472$ ; **Fig. 9H**). We did not observe any significant differences in CBF for the whole brain or cortex.

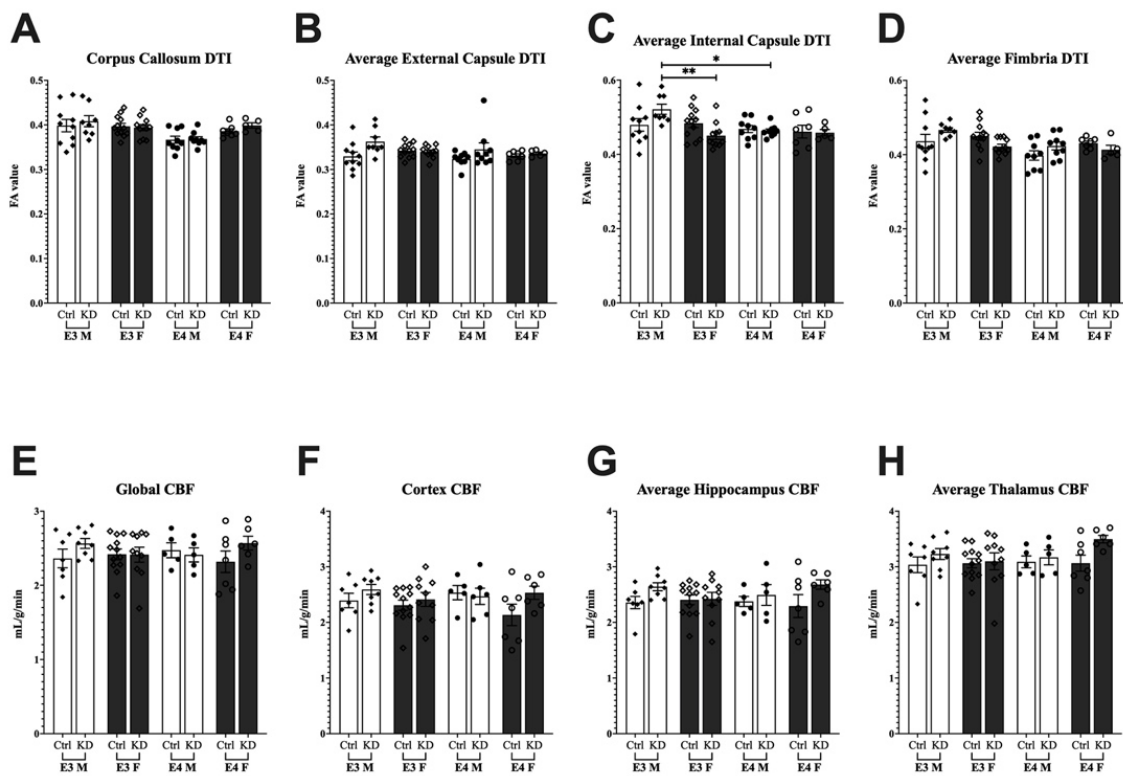


**Figure 9. Sex effects in DTI and CBF measures.** FA values for (A) corpus callosum, (B) averaged left and right external capsule, (C) averaged internal capsule, and (D) averaged fimbria. CBF values for (E) whole brain (global), (F) cortex, (G) averaged hippocampi, and (H) averaged thalamus. \*  $p < 0.05$ ; \*\*  $p < 0.01$ .

### 3.2.5. Sex and diet heavily modified SCFA production and transport.

We observed significant genotype effects only in plasma butyric acid levels ( $F(1,48) = 6.619$ ,  $p = 0.0132$ , **Fig. 10A**). Post-hoc analysis revealed significantly elevated plasma butyric acid in E4-KD females compared to E3-KD females ( $p = 0.0063$ ; **Fig. 10A**). We noted significant diet effects in plasma acetic acid levels ( $F(1,48) = 113.6$ ;  $p < 0.0001$ ; **Fig. 10B**). Post-hoc analysis showed elevated plasma acetic acid across all groups for E3-KD males ( $p = 0.0005$ ), E3-KD females ( $p = 0.0004$ ), E4-KD males ( $p < 0.0001$ ), and E4-KD females ( $p < 0.0001$ ) compared to respective controls (**Fig. 10B**). We observed significant sex effects influenced plasma propionic acid levels ( $F(1,45) = 6.292$ ;  $p = 0.0158$ ; **Fig 7C**). Post-hoc analysis did not show any specific significant differences between groups. We noted significant diet effects ( $F(1,46) = 13.42$ ;  $p = 0.0006$ ), genotype effects ( $F(1,46) = 5.305$ ;  $p = 0.025$ ), and sex effects ( $F(1,46) = 7.612$ ;  $p = 0.0063$ ) in plasma valeric acid levels (**Fig. 10D**). Post-hoc analysis revealed the E4-KD females drove these effects; plasma acetic acid was significantly elevated in E4-KD females compared to E4-Ctrl females ( $p < 0.0001$ ), E3-KD females ( $p = 0.0161$ ), and E4-KD males ( $p = 0.0008$ ; **Fig. 10D**).

We also analyzed the contents of the cecum to identify differences in SCFA production and formation. We noted significant diet effects ( $F(1,51) = 10.98$ ;  $p = 0.0017$ ), genotype effects ( $F(1,51) = 7.213$ ;  $p = 0.0097$ ), and sex effects ( $F(1,51) = 73.18$ ;  $p < 0.0001$ ; **Fig. 10E**) in levels of cecal butyric acid. Post-hoc analysis of cecal butyric acid revealed significantly increased production in the cecum of E3-KD males ( $p = 0.0242$ ) and E4-KD males ( $p = 0.0016$ ) compared to respective controls. Post-hoc analysis of cecal butyric acid also showed significantly increased production in E3-Ctrl males ( $p < 0.0001$ ), E3-KD males ( $p = 0.0145$ ), and E4-Ctrl males ( $p < 0.0001$ ) compared to respective female groups. We did not see significant differences for cecal butyric acid between specific genotype comparisons.

We observed the presence of significant diet effects ( $F(1,51) = 4.266$ ;  $p = 0.0440$ ), genotype effects ( $F(1,51) = 7.213$ ;  $p = 0.0199$ ), and sex effects ( $F(1,51) = 95.15$ ;  $p < 0.0001$ ; **Fig. 10F**) for acetic acid levels in the cecum. Post-hoc analysis of diet effects showed E4-KD males had significantly increased acetic acid relative to E4-Ctrl males ( $p = 0.0192$ ). No significant genotype comparisons were found during post-hoc analysis,

however, post-hoc analysis of sex effects revealed significantly increased acetic acid in cecum of E3-Ctrl males ( $p < 0.0001$ ) and E3-KD males ( $p < 0.0001$ ) relative to respective female groups. We also observed a significant increase in E4-Ctrl males relative to E4-Ctrl females ( $p = 0.0001$ ).

We noted significant genotype effects ( $F(1,49) = 6.578$ ;  $p = 0.0134$ ) and sex effects ( $F(1,49) = 35.56$ ;  $p < 0.0001$ ; **Fig. 10G**) for levels of cecum propionic acid. Post-hoc analysis showed no significant genotype comparisons, though analysis of the sex effects showed increased cecum acetic acid in E3-Ctrl males ( $p = 0.0010$ ) and E3-KD males ( $p = 0.0005$ ) relative to respective female groups.

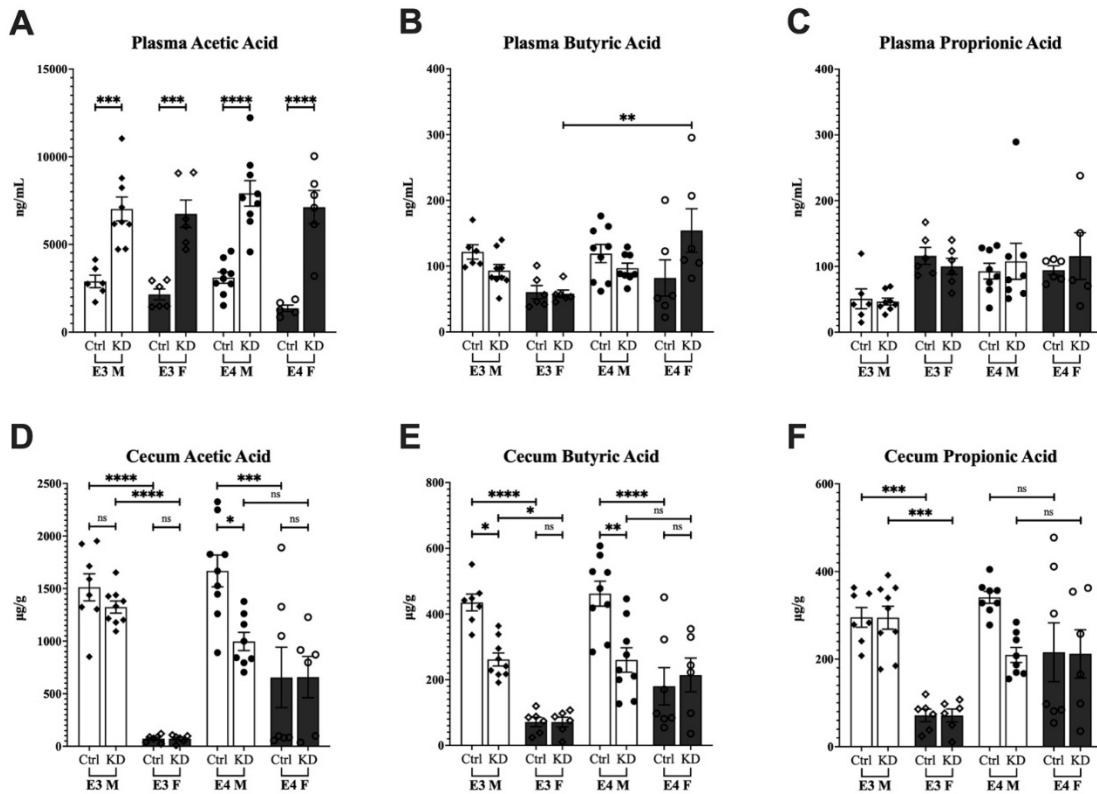


**Figure 10. Sex effects on plasma and cecum SCFA levels.** The top panels, from left to right, display (A) plasma butyric acid levels, (B) plasma acetic acid levels, and (C) plasma propionic acid levels in diet and genotype groups stratified by sex. The bottom panels, from left to right, display (D) cecum butyric acid levels, (E) cecum acetic acid levels, and (F) cecum propionic acid

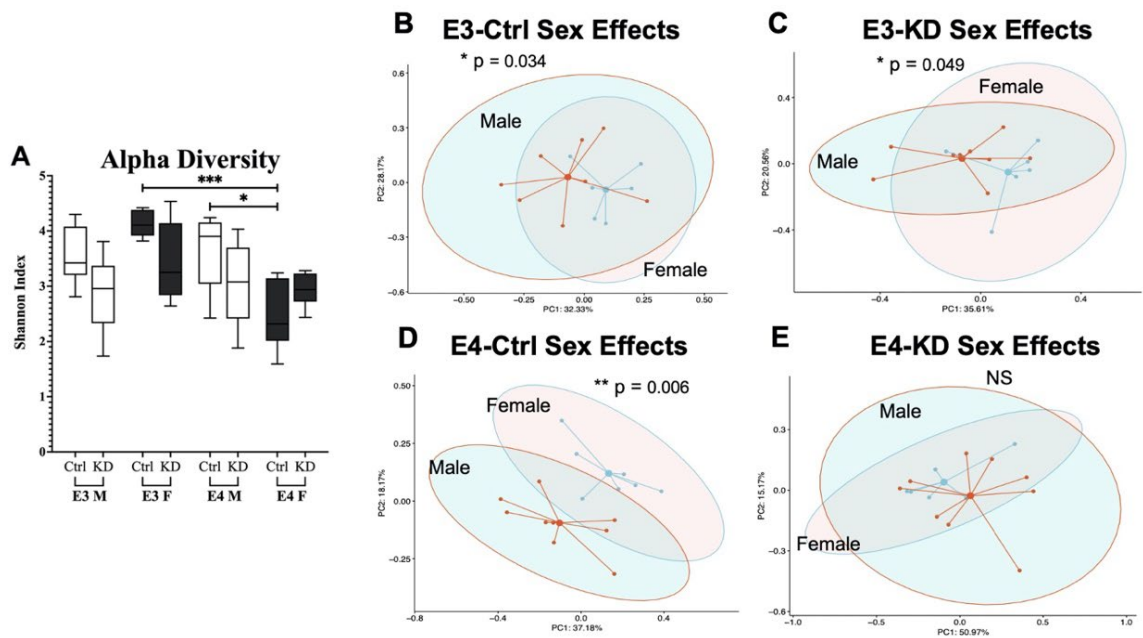


levels in diet and genotype groups stratified by sex. \*  $p < 0.05$ ; \*\*  $p < 0.01$ ; \*\*\*  $p < 0.001$ ; \*\*\*\*  $p < 0.0001$ .

### 3.2.6. Sex disparately altered gut microbial species diversity in E4 male and female mice.

We noted the presence of significant diet effects ( $F(1,52) = 5.171$ ;  $p = 0.0271$ ) and significant genotype effects ( $F(1,52) = 9.713$ ;  $p = 0.0030$ ) in alpha diversity (Shannon index; **Fig. 11A**). Although sex effects were not significant in the ANOVA test, post-hoc analysis showed significantly increased diversity in E4-Ctrl males compared to the E4-Ctrl females ( $p = 0.0066$ , **Fig. 11A**). Post-hoc analysis also revealed significantly increased diversity in E3-Ctrl females compared to E4-Ctrl females ( $p = 0.0001$ ; **Fig. 11A**).

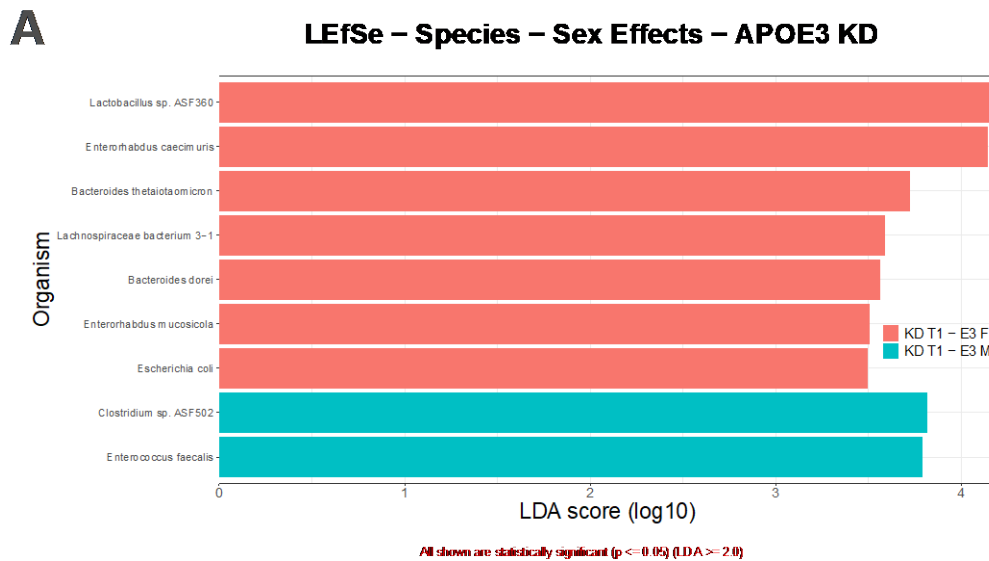
We observed significant sex effects present for beta diversity measures of gut microbial dissimilarity (Bray-Curtis index) between both E3-Ctrl males and females ( $F(1,60) = 2.430$ ;  $p = 0.034$ ; **Fig. 11B**) and between E3-KD males and females ( $F(1,60) = 2.238$ ;  $p = 0.049$ ; **Fig. 8C**). We also observed significant dissimilarity between E4-Ctrl male and female gut microbiota ( $F(1,60) = 3.622$ ;  $p = 0.006$ ; **Fig. 11D**), but not between the E4-KD male and female gut microbiome (**Fig. 11E**).



**Figure 11. Sex effects on alpha and beta diversity. (A)** Alpha diversity (Shannon index) was reduced in E4-Ctrl females. Beta diversity (Bray-Curtis index) comparisons revealed significant dissimilarity between the gut microbial communities of **(B)** E3-Ctrl males and females, **(C)** E3-KD males and females, and **(D)** E4-Ctrl males and females. E4-KD males and females did not have significant dissimilarity in the gut microbiome. \*  $p < 0.05$ ; \*\*  $p < 0.01$ ; \*\*\*  $p < 0.001$ .

### 3.2.7. Sex contributed to differences between gut microbial profiles in both E3 and E4 mice.

We observed significant sex effects between E3-KD, E3-Ctrl and E4-KD groups (**Fig. 12A, 12B, 12C**, respectively). We found that, in the E3 groups, the males and females had significantly dissimilar gut microbiomes; an effect that diet did not normalize between the different sexes. The E3-KD males had significantly different gut microbial profiles when compared to E3-KD females (**Fig. 12A**;  $p < 0.05$ ), as did the E3-Ctrl males compared to E3-Ctrl females (**Fig. 12B**;  $p < 0.05$ ). Contrarily, we found significant dissimilarity between the E4-Ctrl male and female gut microbiota populations only (**Fig. 12C**;  $p < 0.01$ ). The KD diet reduced this sex difference below significance.



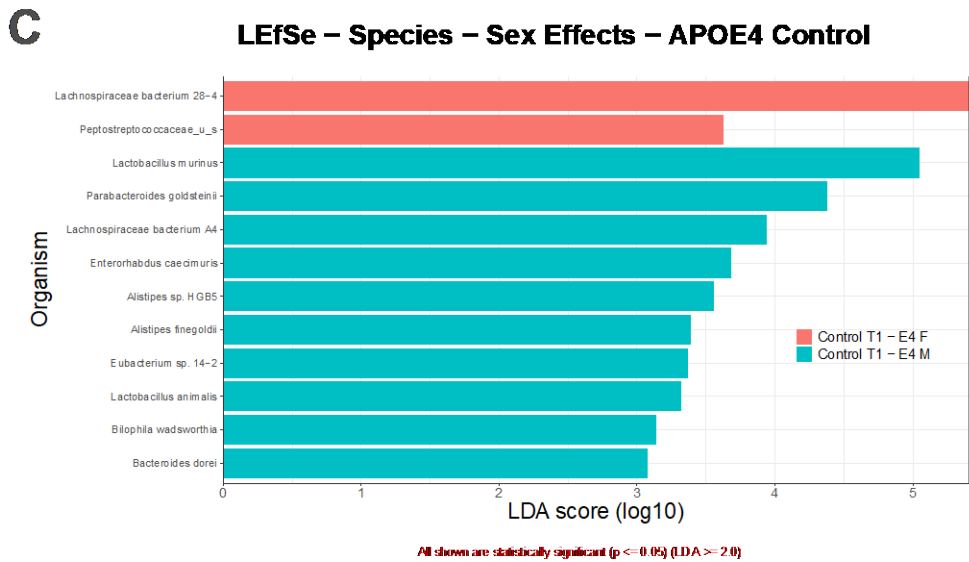
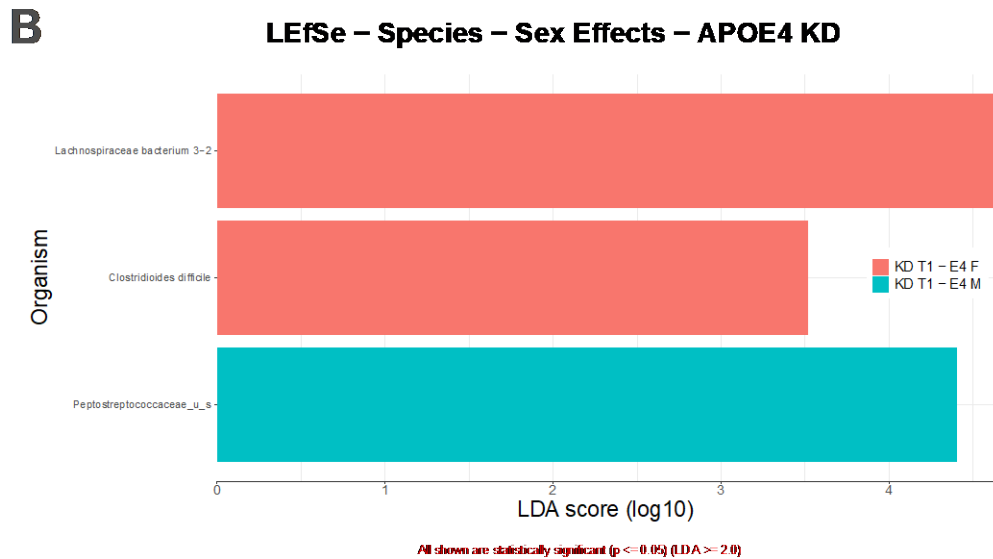


**Figure 12. Sex effects on gut microbial composition.** The LEfSe figures display microbial species that were significantly different between sexes for groups (A) E3-KD, (B) E3-Ctrl, and (C) E4-Ctrl.

**Table 7.** Results summary table.

<i>Parameter</i>	<b>APOE3-KD</b>	<b>APOE4-KD</b>
<i>Body weight</i>	Similar reductions in body weight	
<i>Caloric intake</i>	Similar increases in caloric intake	
<i>Blood Glucose Levels</i>	Reduced glycolysis (or reduced glucose levels)	
<i>Blood Ketone Body Levels</i>	Induced ketogenesis	
<i>SCFA's</i>	Enhanced short chain fatty acid production	
<i>Gut Microbiome</i>	Increases in Firmicutes relative to Bacteroidetes	
<i>Alpha Diversity</i>	KD normalized alpha diversity	
<i>Beta Diversity</i>	KD did not normalize beta diversity	KD normalized beta diversity
<i>Microbiome LEfSe</i>	KD promoted healthier microbial species growth	

#### 4. DISCUSSION

This study provides evidence for the KD as a preventative therapy for AD in young APOE3 and APE4 male and female transgenic mouse models. Specifically, KD intervention in young male and female APOE transgenic mice can decrease body weight, reduce glucose utilization, enhance TCA cycle flux and antioxidant protection, restore brain metabolites involved in neurotransmitter synthesis and neuronal integrity, normalize fatty acid levels, and enhance short chain fatty acid production, utilization, and exportation to periphery. Furthermore, we show that KD beneficially alters the gut

microbiome by promoting the growth of healthy microbial species, and normalizing alpha and beta diversity.

The APOE4 allele increases risk for sporadic AD in part due to the pathological metabolic and vascular deficits that arise decades before the onset of clinical symptoms (2021). One mechanism through which these pathological changes are thought to contribute to AD development is by promoting systemic dysregulation of energy homeostasis, resulting in chronic cellular energy deficit that leads to increased reactive oxygen species (ROS), inflammation, and cell death (de la Monte and Tong, 2014). In line with this, we report evidence of a dysregulated metabolism in APOE4 mice fed a control diet relative to APOE3 mice fed the same diet: E4-Ctrl mice had significantly reduced cortical levels of most primary TCA cycle intermediates and several amino acids and their intermediates, such as neurotransmitters GABA, glutamate, and glutamine. The E4-Ctrl mice also had significantly increased cortical levels of oxidized glutathione, a biomarker of high mitochondrial oxidative stress, relative to the E3-Ctrl mice. Myelination also appeared to be subject to genotype effects, as E4-Ctrl mice displayed significantly reduced myelin content in the corpus callosum and fimbria relative to E3-Ctrl mice, as shown by DTI scan. The E4 allele is thought to contribute to demyelination, potentially through interaction with the mammalian Target of Rapamycin (mTOR) protein complex, though the full mechanisms are unknown. We also report similar weights between the E4-Ctrl and E3-Ctrl groups. Prior studies have shown APOE4-TR mice have reduced weight on chow diets relative to APOE3-TR mice (Huebbe et al., 2015; Lane-Donovan and Herz, 2016), though this difference appears to increase with age. Our study investigated the effects of dietary intervention on young mice (~9 months old at sacrifice), which could explain the differing results.

It is also becoming increasingly clear that, in addition to genetic risk factors like the E4 allele, modifiable lifestyle factors such as diet and exercise can also contribute to or reduce the risk of sporadic AD (Norwitz et al., 2021). The KD dietary intervention in APOE4-TR mice significantly improved the metabolic dysregulation seen in E4 mice – we report increases in E4-KD cortical amino acid metabolites, including neurotransmitters GABA, glutamine, and glutamate, along with a normalization of TCA cycle intermediates and the antioxidant glutathione pool relative to E4-Ctrl mice. We also

report a significant weight reduction and significant plasma ketone body levels in E4-KD mice relative to E4-Ctrl. Previous studies in both APOE-TR and wildtype (WT) mice have similarly shown KD-induced reductions in weight (Lane-Donovan and Herz, 2016; Ma et al., 2018) and increases in plasma ketone bodies (Ma et al., 2018). Further diet effects from KD intervention include significant increases in plasma SCFA's (butyric acid, acetic acid), along with significant increases in *Firmicutes*, a phyla consisting of species known to produce SCFA's, such as *Lactobacillus* (Ma et al., 2018). Lastly, we report a significant shift in gut microbial community composition ( $\beta$ -diversity, Bray-Curtis index) driven by KD intervention in E4 mice relative to E4 mice on control die. A similar study in young, WT mice also reports a KD-induced shift in the gut microbial community (Ma et al., 2018).

We also report a similar metabolic enhancement in APOE3 mice fed the KD, relative to E3 mice fed a Control diet. Notably, we report a reduction in multiple carbohydrate and amino acid metabolic intermediates in the cortices of E3-KD mice relative to E3-Ctrl, where the reverse was true among the E4 comparison. On the other hand, KD altered the E3 gut microbial community more robustly than it did for the E4 mice, though both the E3-KD and E4-KD had significantly dissimilar gut composition relative to respective controls. Although, the E3-KD did experience significantly enhanced F:B ratio relative to E3-Ctrl, as well as significantly increased relative abundance of *Bacteroidetes spp.*, *Firmicutes spp.*, and *Proteobacteria spp.*

There is a profound lack of research focusing on the interaction between APOE and sex, especially considering our results. E4 female mice experienced remarkable recovery from KD intervention in a variety of health parameters, including metabolomics, gut microbiome, plasma SCFA's, and CBF. The E4 male mice and E4 female mice experienced similar improvements from KD intervention, though females displayed a far more robust response to the KD. The results of this study allude to an interplay between APOE genotype and sex that can affect many various aspects of health, especially gut microbiome composition and energy metabolism. The results are broken down into two separate sections. The first section focuses only on diet and genotype effects, and the results indicate that the KD diet was beneficial to both E3 and E4 mice; while the health improvements to E3 were minimal, the E4 mice had considerable restoration of health

measures with KD intervention. The second section further splits the data to include sex, and this reveals that the E4 female mice suffer the most from APOE4-associated health deficits. However, again, incredible restoration of health measures is seen with KD intervention. In summary, our results demonstrate three key findings: 1) the E4 allele presents a multifaceted detrimental phenotype in both males and females, 2) this negative health phenotype is more pronounced in females than in males, and 3) the KD can help restore the phenotype regardless of sex, and even improve the comparatively healthier E3 phenotype.

This study is not without its limitations. The main limitation is the relatively small sample size, especially of the E4 female cohort, which became a stronger focus of this study than expected. Due to the exploratory nature of our study, we chose to focus on KD effects in young mice, even though a more aged study population would have very likely increased significances between comparisons. However, our findings offer a priori hypotheses to be tested in more expansive, future studies. Other studies focusing on dietary intervention in APOE-TR mice accounted for homozygotic and heterozygotic APOE status (Lane-Donovan and Herz, 2016). We did not consider zygosity for the human/wildtype APOE alleles, thus, we are unable to determine how significantly zygosity contributed to the results. Another important limitation is that we failed to control for a fed or fasted state prior to MRI scans or tissue collection. The difference between metabolite concentrations, SCFA production and utilization, CBF, gut microbiome and other many other measures depend heavily on energetic status and may fluctuate immensely as the body changes from one nutritional state to the other, potentially affecting results.

Future research focusing on dietary and lifestyle interventions for early AD prevention should seek to elucidate the specific mechanisms of peripheral and neuronal APOE response to a ketogenic diet, along with other dietary and lifestyle interventions. An emphasis should be placed on specific gene expression profiles involved in metabolic function, especially in relation to sex chromosomal influences on metabolism. Peripheral and CNS APOE expression differ relative to each other and respond to dietary and lifestyle habits through an interplay between the two distinct pools, thus, future research

should investigate the pathways through which these related APOE pools interact and how strongly they can influence each other.

In this study, we detail how a dietary intervention with KD can effectively alter the gut microbiome in a young, transgenic AD mouse model, enhance neural metabolic functions and sustain a healthy body weight. We focus on the underlying metabolic features contributed by the APOE4 genotype, the largest genetic risk factor for the development of AD and show how KD intervention can help mitigate APOE4-related health deficits. This represents a shift in AD research, from the amyloid hypothesis to the metabolic features underlying the disease. As impairment of energy metabolism and elevation of neuroinflammation are well-established features of AD, a nutritional approach that engenders a fundamental shift in systemic metabolism could provide a viable strategy to reverse the E4-related health risks and prevent the onset of the disease. Understanding the dietary effects in the context of the gut-brain axis may have significant future implications for preventing AD in asymptomatic APOE4 carriers.



## APPENDIX

### Metabolon Platform

**Sample Accessioning:** Following receipt, samples were inventoried and immediately stored at -80°C. Each sample received was accessioned into the Metabolon LIMS system and was assigned by the LIMS a unique identifier that was associated with the original source identifier only. This identifier was used to track all sample handling, tasks, results, etc. The samples (and all derived aliquots) were tracked by the LIMS system. All portions of any sample were automatically assigned their own unique identifiers by the LIMS when a new task was created; the relationship of these samples was also tracked. All samples were maintained at -80°C until processed.

**Sample Preparation:** Samples were prepared using the automated MicroLab STAR® system from Hamilton Company. Several recovery standards were added prior to the first step in the extraction process for QC purposes. To remove protein, dissociate small molecules bound to protein or trapped in the precipitated protein matrix, and to recover chemically diverse metabolites, proteins were precipitated with methanol under vigorous shaking for 2 min (Glen Mills GenoGrinder 2000) followed by centrifugation. The resulting extract was divided into five fractions: two for analysis by two separate reverse phase (RP)/UPLC-MS/MS methods with positive ion mode electrospray ionization (ESI), one for analysis by RP/UPLC-MS/MS with negative ion mode ESI, one for analysis by HILIC/UPLC-MS/MS with negative ion mode ESI, and one sample was reserved for backup. Samples were placed briefly on a TurboVap® (Zymark) to remove the organic solvent. The sample extracts were stored overnight under nitrogen before preparation for analysis.

**QA/QC:** Several types of controls were analyzed in concert with the experimental samples: a pooled matrix sample generated by taking a small volume of each experimental sample (or alternatively, use of a pool of well-characterized human plasma) served as a technical replicate throughout the data set; extracted water samples served as process blanks; and a cocktail of QC standards that were carefully chosen not to interfere with the measurement of endogenous compounds were spiked into every analyzed sample, allowed

instrument performance monitoring and aided chromatographic alignment. Tables 8 and 9 describe these QC samples and standards. Instrument variability was determined by calculating the median relative standard deviation (RSD) for the standards that were added to each sample prior to injection into the mass spectrometers. Overall process variability was determined by calculating the median RSD for all endogenous metabolites (i.e., non-instrument standards) present in 100% of the pooled matrix samples. Experimental samples were randomized across the platform run with QC samples spaced evenly among the injections, as outlined in Figure 13.

**Table 8:** Description of Metabolon QC Samples

Type	Description	Purpose
MTRX	Large pool of human plasma maintained by Metabolon that has been characterized extensively.	Assure that all aspects of the Metabolon process are operating within specifications.
CMTRX	Pool created by taking a small aliquot from every customer sample.	Assess the effect of a non-plasma matrix on the Metabolon process and distinguish biological variability from process variability.
PRCS	Aliquot of ultra-pure water	Process Blank used to assess the contribution to compound signals from the process.
SOLV	Aliquot of solvents used in extraction.	Solvent Blank used to segregate contamination sources in the extraction.

**Table 9:** Metabolon QC Standards

Type	Description	Purpose
RS	Recovery Standard	Assess variability and verify performance of extraction and instrumentation.
IS	Internal Standard	Assess variability and performance of instrument.

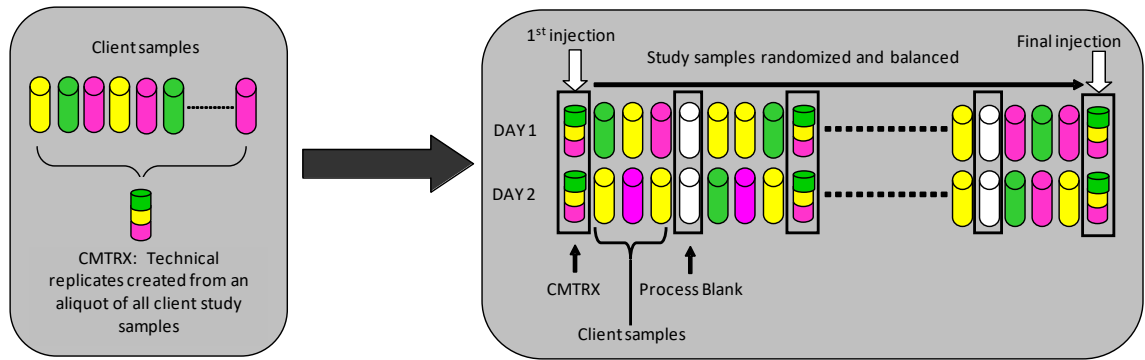


**Figure 13. Preparation of client-specific technical replicates.** A small aliquot of each client sample (colored cylinders) is pooled to create a CMTRX technical replicate sample (multi-colored cylinder), which is then injected periodically throughout the platform run. Variability among consistently detected biochemicals can be used to calculate an estimate of overall process and platform variability.

**Ultrahigh Performance Liquid Chromatography-Tandem Mass Spectroscopy (UPLC-MS/MS):** All methods utilized a Waters ACQUITY ultra-performance liquid chromatography (UPLC) and a Thermo Scientific Q-Exactive high resolution/accurate mass spectrometer interfaced with a heated electrospray ionization (HESI-II) source and Orbitrap mass analyzer operated at 35,000 mass resolution. The sample extract was dried then reconstituted in solvents compatible to each of the four methods. Each reconstitution solvent contained a series of standards at fixed concentrations to ensure injection and chromatographic consistency. One aliquot was analyzed using acidic positive ion conditions, chromatographically optimized for more hydrophilic compounds. In this method, the extract was gradient eluted from a C18 column (Waters UPLC BEH C18-2.1x100 mm, 1.7  $\mu$ m) using water and methanol, containing 0.05% perfluoropentanoic acid (PFPA) and 0.1% formic acid (FA). Another aliquot was also analyzed using acidic positive ion conditions, however it was chromatographically optimized for more hydrophobic compounds. In this method, the extract was gradient eluted from the same afore mentioned C18 column using methanol, acetonitrile, water, 0.05% PFPA and 0.01% FA and was operated at an overall higher organic content. Another aliquot was analyzed using basic negative ion optimized conditions using a separate dedicated C18 column. The basic extracts were gradient eluted from the column using methanol and water, however with 6.5mM Ammonium Bicarbonate at pH 8. The fourth aliquot was analyzed via negative ionization following elution from a HILIC column (Waters UPLC BEH Amide 2.1x150 mm, 1.7  $\mu$ m) using a gradient consisting of water and acetonitrile with 10mM Ammonium Formate, pH 10.8. The MS analysis alternated between MS and data-dependent MS<sup>n</sup> scans using dynamic exclusion. The scan range varied slightly between methods but covered 70-1000 m/z. Raw data files are archived and extracted as described below.

**Bioinformatics:** The informatics system consisted of four major components, the Laboratory Information Management System (LIMS), the data extraction and peak-identification software, data processing tools for QC and compound identification, and a collection of information interpretation and visualization tools for use by data analysts. The hardware and software foundations for these informatics components were the LAN backbone, and a database server running Oracle 10.2.0.1 Enterprise Edition.

**LIMS:** The purpose of the Metabolon LIMS system was to enable fully auditable laboratory automation through a secure, easy to use, and highly specialized system. The scope of the Metabolon LIMS system encompasses sample accessioning, sample preparation and instrumental analysis and reporting and advanced data analysis. All of the subsequent software systems are grounded in the LIMS data structures. It has been modified to leverage and interface with the in-house information extraction and data visualization systems, as well as third party instrumentation and data analysis software.

**Data Extraction and Compound Identification:** Raw data was extracted, peak-identified and QC processed using Metabolon's hardware and software. These systems are built on a web-service platform utilizing Microsoft's .NET technologies, which run on high-performance application servers and fiber-channel storage arrays in clusters to provide active failover and load-balancing. Compounds were identified by comparison to library entries of purified standards or recurrent unknown entities. Metabolon maintains a library based on authenticated standards that contains the retention time/index (RI), mass to charge ratio ( $m/z$ ), and chromatographic data (including MS/MS spectral data) on all molecules present in the library. Furthermore, biochemical identifications are based on three criteria: retention index within a narrow RI window of the proposed identification, accurate mass match to the library +/- 10 ppm, and the MS/MS forward and reverse scores between the experimental data and authentic standards. The MS/MS scores are based on a comparison of the ions present in the experimental spectrum to the ions present in the library spectrum. While there may be similarities between these molecules based on one of these factors, the use of all three data points can be utilized to distinguish and differentiate biochemicals. More than 3300 commercially available purified standard compounds have been acquired and registered into LIMS for analysis on all platforms for determination of their analytical characteristics. Additional mass spectral entries have been created for structurally unnamed biochemicals, which have been identified by virtue of their recurrent nature (both chromatographic and mass spectral). These compounds have the potential to be identified by future acquisition of a matching purified standard or by classical structural analysis.

**Curation:** A variety of curation procedures were carried out to ensure that a high quality data set was made available for statistical analysis and data interpretation. The QC and curation processes were designed to ensure accurate and consistent identification of true chemical entities, and to remove those representing system artifacts, mis-assignments, and background noise. Metabolon data analysts use proprietary visualization and interpretation software to confirm the consistency of peak identification among the various samples. Library matches for each compound were checked for each sample and corrected if necessary.

**Metabolite Quantification and Data Normalization:** Peaks were quantified using area-under-the-curve. For studies spanning multiple days, a data normalization step was performed to correct variation resulting from instrument inter-day tuning differences. Essentially, each compound was corrected in run-day blocks by registering the medians to equal one (1.00) and normalizing each data point proportionately (termed the “block correction”; Figure 14). For studies that did not require more than one day of analysis, no normalization is necessary, other than for purposes of data visualization. In certain instances, biochemical data may have been normalized to an additional factor (e.g., cell counts, total protein as determined by Bradford assay, osmolality, etc.) to account for differences in metabolite levels due to differences in the amount of material present in each sample.

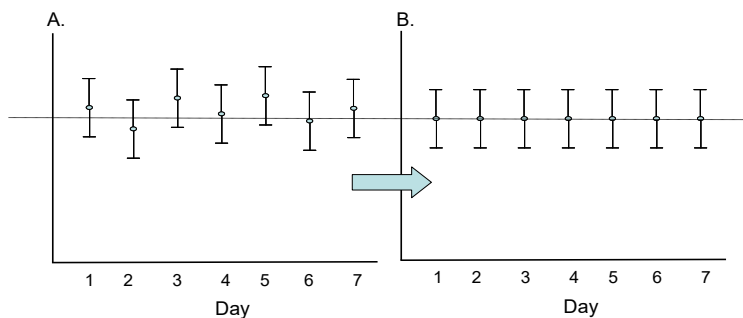


**Figure 14: Visualization of data normalization steps for a multiday platform run.**

## Statistical Methods and Terminology

**Statistical Calculations:** For many studies, two types of statistical analysis are usually performed: (1) significance tests and (2) classification analysis. Standard statistical analyses are performed in ArrayStudio on log transformed data. For those analyses not standard in ArrayStudio, the programs R (<http://cran.r-project.org/>) or JMP are used. Below are examples of frequently employed significance tests and classification methods followed by a discussion of p- and q-value significance thresholds.

### 1. One-way ANOVA

ANOVA stands for analysis of variance. For ANOVA, it is assumed that all populations have the same variances. One-way ANOVA is used to test whether at least two unknown means are all equal or whether at least one pair of means is different. For the case of two means, ANOVA gives the same result as a two-sided *t*-test with a pooled estimate of the variance.

An ANOVA uses an F-test which has two parameters – the numerator degrees of freedom and the denominator degrees of freedom. The degrees of freedom in the numerator are equal to  $g - 1$ , where  $g$  is the number of groups. If  $n$  is the total number of observations ( $n_1 + n_2$ ), then, the denominator degrees of freedom is equal to  $n - g$ . The F-statistic is the ratio of the between-groups variance to the within-groups variance, hence the higher the F-statistic the more evidence we have that the means are different.

Often within ANOVA, one performs linear contrasts for specific comparisons of interest. For example, suppose we have three groups A, B, C, then examples of some contrasts are A vs. B, the average of A and B vs. C, etc. For single-degree of freedom contrasts, these give the same result as a two-sided *t*-test with the pooled estimate of the variance from the ANOVA and degrees of freedom  $n - g$ . Below, we show the three formulas for A vs. B from a three group design as shown above. The numerator is same in each case, but the denominator differs by the estimates of the variances, and the degrees of freedom are different for each (if the theoretical

assumptions hold, then the contrast has the most power, as it has the largest degrees of freedom).

Welch's two-sample  $t$ -test

By  $t = (\bar{x}_A - \bar{x}_B) / \sqrt{s_A^2/n_A + s_B^2/n_B}$ , and the degrees of freedom is given by

$$\left(\frac{s_A^2}{n_A} + \frac{s_B^2}{n_B}\right)^2 / \left(\frac{\left(\frac{s_A^2}{n_A}\right)^2}{n_A-1} + \frac{\left(\frac{s_B^2}{n_B}\right)^2}{n_B-1}\right)$$

Two-sample  $t$ -test with pooled estimate of variance from A and B

$$t = (\bar{x}_A - \bar{x}_B) / \sqrt{s_{AB}^2(1/n_A + 1/n_B)}$$

where  $s_{AB}^2 = ((n_A - 1)s_A^2 + (n_B - 1)s_B^2) / (n_A + n_B - 2)$ , where the degrees of freedom is  $n_A + n_B - 2$ .

The contrast from the ANOVA,

$$t = (\bar{x}_A - \bar{x}_B) / \sqrt{s^2(1/n_A + 1/n_B)}$$

where  $s^2 = ((n_A - 1)s_A^2 + (n_B - 1)s_B^2 + (n_C - 1)s_C^2) / (n_A + n_B + n_C - 3)$ , where the degrees of freedom is given by where the degrees of freedom is  $n_A + n_B + n_C - 3$ .

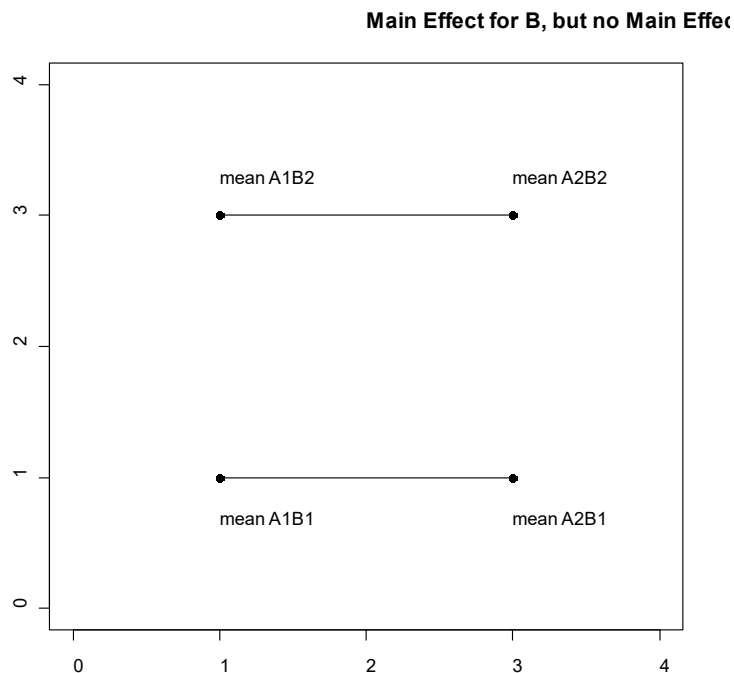
## 2. Two-way ANOVA

ANOVA stands for analysis of variance. For ANOVA, it is assumed that all populations have the same variances. For a two-way ANOVA, three statistical tests are typically performed: the main effect of each factor and the interaction. Suppose we have two factors A and B, where A represent the genotype and B represent the diet in a mouse study. Suppose each of these factors has two levels (A: wild type, knock out; B: standard diet, high fat diet). For this example, there are 4 combinations ("treatments"): A1B1, A1B2, A2B1, A2B2. The overall ANOVA F-test gives the p-value for testing whether all four of these means are equal or whether at least one pair is different. However, we are also interested in the effect of the genotype and diet. A main effect is a contrast that tests one factor

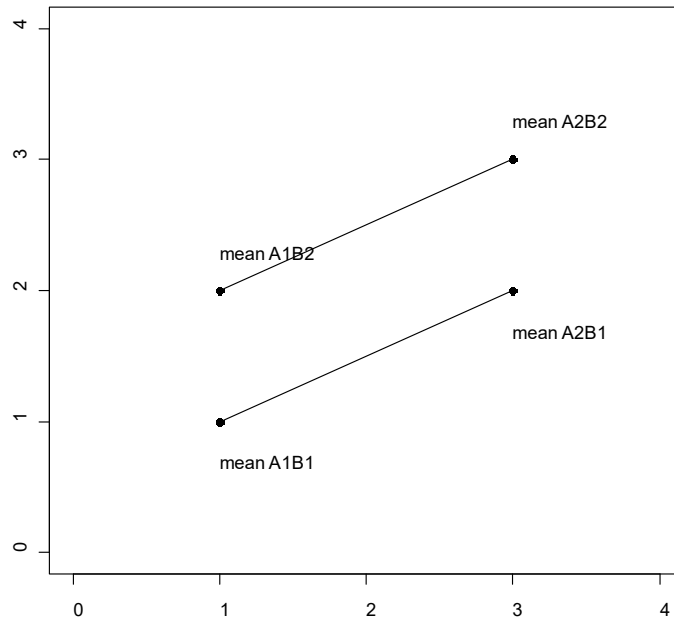


across the levels of the other factor. Hence the A main effect compares  $(A1B1 + A1B2)/2$  vs.  $(A2B1 + A2B2)/2$ , and the B-main effect compares  $(A1B1 + A2B2)/2$  vs.  $(A1B2 + A2B1)/2$ . The interaction is a contrast that tests whether the mean difference for one factor depends on the level of the other factor, which is  $(A1B2 + A2B1)/2$  vs.  $(A1B1 + A2B2)/2$ .

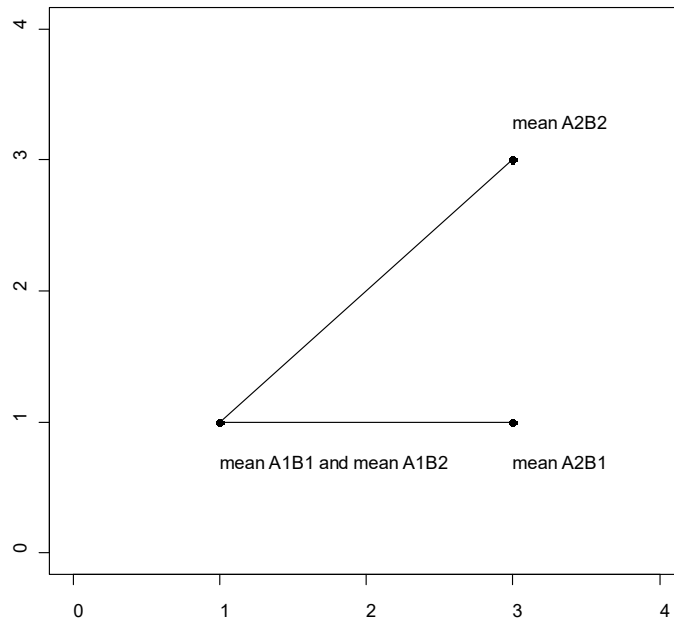
Some sample plots follow. For the first plot, there is a B main effect, but no A main effect and no interaction, as the effect of B does not depend on the level of A. For the second plot, notice how the mean difference for B is the same at each level of A and the difference in A is the same for each level of B, hence there is no statistical interaction. The final plot also has main effects for A and B, but here also has an interaction: we see the effect of B depends on the level of A (0 for A1 but 2 for A2), i.e., the effect of the diet depends on the genotype. We also see here the interpretation of the main effects depends on whether there is an interaction or not.



Main Effect for A, Main Effect for B,



Main Effect for A, Main Effect for B,



**p- values**

For statistical significance testing, p-values are given. The lower the p-value, the more evidence we have that the null hypothesis (typically that two population

means are equal) is not true. If “statistical significance” is declared for p-values less than 0.05, then 5% of the time we incorrectly conclude the means are different, when actually they are the same.

The p-value is the probability that the test statistic is at least as extreme as observed in this experiment given that the null hypothesis is true. Hence, the more extreme the statistic, the lower the p-value and the more evidence the data gives against the null hypothesis.

### **q-values**

The level of 0.05 is the false positive rate when there is one test. However, for a large number of tests we need to account for false positives. There are different methods to correct for multiple testing. The oldest methods are family-wise error rate adjustments (Bonferroni, Tukey, etc.), but these tend to be extremely conservative for a very large number of tests. With gene arrays, using the False Discovery Rate (FDR) is more common. The family-wise error rate adjustments give one a high degree of confidence that there are zero false discoveries. However, with FDR methods, one can allow for a small number of false discoveries. The FDR for a given set of compounds can be estimated using the q-value (see Storey J and Tibshirani R. (2003) Statistical significance for genomewide studies. Proc. Natl. Acad. Sci. USA 100: 9440-9445; PMID: 12883005).

In order to interpret the q-value, the data must first be sorted by the p-value then choose the cutoff for significance (typically  $p < 0.05$ ). The q-value gives the false discovery rate for the selected list (i.e., an estimate of the proportion of false discoveries for the list of compounds whose p-value is below the cutoff for significance). For Table 1 below, if the whole list is declared significant, then the false discovery rate is approximately 10%. If everything from Compound 079 and above is declared significant, then the false discovery rate is approximately 2.5%.

**Table 10:** Example of q-value interpretation

Compound	p-value	q-value
Compound 103	0.0002	0.0122
Compound 212	0.0004	0.0122
Compound 076	0.0004	0.0122
Compound 002	0.0005	0.0122
Compound 168	0.0006	0.0122
Compound 079	0.0016	0.0258
Compound 113	0.0052	0.0631
Compound 050	0.0053	0.0631
Compound 098	0.0061	0.0647
Compound 267	0.0098	0.0939

### Principal Components Analysis (PCA)

Principal components analysis is an unsupervised analysis that reduces the dimension of the data. Each principal component is a linear combination of every metabolite and the principal components are uncorrelated. The number of principal components is equal to the number of observations.

The first principal component is computed by determining the coefficients of the metabolites that maximizes the variance of the linear combination. The second component finds the coefficients that maximize the variance with the condition that the second component is orthogonal to the first. The third component is orthogonal to the first two components and so on. The total variance is defined as the sum of the variances of the predicted values of each component (the variance is the square of the standard deviation), and for each component, the proportion of the total variance is computed. For example, if the standard deviation of the predicted values of the first principal component is 0.4 and the total variance = 1, then  $100 \times 0.4 \times 0.4 / 1 = 16\%$  of the total variance is explained by the first component. Since this is an unsupervised method, the main components may be unrelated to the treatment groups, and the “separation” does not give an estimate of the true predictive ability.

## REFERENCES

- (2021). 2021 Alzheimer's disease facts and figures. *Alzheimers Dement* 17(3), 327-406. doi: 10.1002/alz.12328.
- Alexander, A.L., Lee, J.E., Lazar, M., and Field, A.S. (2007). Diffusion tensor imaging of the brain. *Neurotherapeutics* 4(3), 316-329. doi: 10.1016/j.nurt.2007.05.011.
- Altmann, A., Tian, L., Henderson, V.W., Greicius, M.D., and Alzheimer's Disease Neuroimaging Initiative, I. (2014). Sex modifies the APOE-related risk of developing Alzheimer disease. *Ann Neurol* 75(4), 563-573. doi: 10.1002/ana.24135.
- Baranano, K.W., and Hartman, A.L. (2008). The ketogenic diet: uses in epilepsy and other neurologic illnesses. *Curr Treat Options Neurol* 10(6), 410-419. doi: 10.1007/s11940-008-0043-8.
- Bostanciklioglu, M. (2019). The role of gut microbiota in pathogenesis of Alzheimer's disease. *J Appl Microbiol* 127(4), 954-967. doi: 10.1111/jam.14264.
- Bozzali, M., Falini, A., Franceschi, M., Cercignani, M., Zuffi, M., Scotti, G., et al. (2002). White matter damage in Alzheimer's disease assessed in vivo using diffusion tensor magnetic resonance imaging. *J Neurol Neurosurg Psychiatry* 72(6), 742-746. doi: 10.1136/jnnp.72.6.742.
- Bredesen, D.E., Amos, E.C., Canick, J., Ackerley, M., Raji, C., Fiala, M., et al. (2016). Reversal of cognitive decline in Alzheimer's disease. *Aging (Albany NY)* 8(6), 1250-1258. doi: 10.18632/aging.100981.
- Broom, G.M., Shaw, I.C., and Rucklidge, J.J. (2019). The ketogenic diet as a potential treatment and prevention strategy for Alzheimer's disease. *Nutrition* 60, 118-121. doi: 10.1016/j.nut.2018.10.003.
- Calsolaro, V., and Edison, P. (2016). Alterations in Glucose Metabolism in Alzheimer's Disease. *Recent Pat Endocr Metab Immune Drug Discov* 10(1), 31-39. doi: 10.2174/1872214810666160615102809.
- Cunnane, S.C., Courchesne-Loyer, A., St-Pierre, V., Vandenberghe, C., Pierotti, T., Fortier, M., et al. (2016). Can ketones compensate for deteriorating brain glucose uptake during aging? Implications for the risk and treatment of Alzheimer's disease. *Annals of the New York Academy of Sciences* 1367(1), 12-20. doi: 10.1111/nyas.12999.
- de la Monte, S.M., and Tong, M. (2014). Brain metabolic dysfunction at the core of Alzheimer's disease. *Biochem Pharmacol* 88(4), 548-559. doi: 10.1016/j.bcp.2013.12.012.
- Evans, A.M., DeHaven, C.D., Barrett, T., Mitchell, M., and Milgram, E. (2009). Integrated, nontargeted ultrahigh performance liquid

- chromatography/electrospray ionization tandem mass spectrometry platform for the identification and relative quantification of the small-molecule complement of biological systems. *Anal Chem* 81(16), 6656-6667. doi: 10.1021/ac901536h.
- Guo, J., Bakshi, V., and Lin, A.L. (2015). Early Shifts of Brain Metabolism by Caloric Restriction Preserve White Matter Integrity and Long-Term Memory in Aging Mice. *Front Aging Neurosci* 7, 213. doi: 10.3389/fnagi.2015.00213.
- Hoffman, J.D., Yanckello, L.M., Chlipala, G., Hammond, T.C., McCulloch, S.D., Parikh, I., et al. (2019). Dietary inulin alters the gut microbiome, enhances systemic metabolism and reduces neuroinflammation in an APOE4 mouse model. *PLoS One* 14(8), e0221828. doi: 10.1371/journal.pone.0221828.
- Hogh, P., Knudsen, G.M., Kjaer, K.H., Jorgensen, O.S., Paulson, O.B., and Waldemar, G. (2001). Single photon emission computed tomography and apolipoprotein E in Alzheimer's disease: impact of the epsilon4 allele on regional cerebral blood flow. *J Geriatr Psychiatry Neurol* 14(1), 42-51. doi: 10.1177/089198870101400110.
- Hotamisligil, G.S. (2006). Inflammation and metabolic disorders. *Nature* 444(7121), 860-867. doi: 10.1038/nature05485.
- Huebbe, P., Dose, J., Schloesser, A., Campbell, G., Gluer, C.C., Gupta, Y., et al. (2015). Apolipoprotein E (APOE) genotype regulates body weight and fatty acid utilization-Studies in gene-targeted replacement mice. *Mol Nutr Food Res* 59(2), 334-343. doi: 10.1002/mnfr.201400636.
- Kennedy, A.R., Pissios, P., Otu, H., Roberson, R., Xue, B., Asakura, K., et al. (2007). A high-fat, ketogenic diet induces a unique metabolic state in mice. *Am J Physiol Endocrinol Metab* 292(6), E1724-1739. doi: 10.1152/ajpendo.00717.2006.
- Lane, C.A., Hardy, J., and Schott, J.M. (2018). Alzheimer's disease. *Eur J Neurol* 25(1), 59-70. doi: 10.1111/ene.13439.
- Lane-Donovan, C., and Herz, J. (2016). High-Fat Diet Changes Hippocampal Apolipoprotein E (ApoE) in a Genotype- and Carbohydrate-Dependent Manner in Mice. *PLoS One* 11(2), e0148099. doi: 10.1371/journal.pone.0148099.
- Lin, A.L., Zhang, W., Gao, X., and Watts, L. (2015). Caloric restriction increases ketone bodies metabolism and preserves blood flow in aging brain. *Neurobiol Aging* 36(7), 2296-2303. doi: 10.1016/j.neurobiolaging.2015.03.012.
- Ma, D., Wang, A.C., Parikh, I., Green, S.J., Hoffman, J.D., Chlipala, G., et al. (2018). Ketogenic diet enhances neurovascular function with altered gut microbiome in young healthy mice. *Sci Rep* 8(1), 6670. doi: 10.1038/s41598-018-25190-5.
- Maalouf, M., Rho, J.M., and Mattson, M.P. (2009). The neuroprotective properties of calorie restriction, the ketogenic diet, and ketone bodies. *Brain Res Rev* 59(2), 293-315. doi: 10.1016/j.brainresrev.2008.09.002.

- Matsuda, H. (2001). Cerebral blood flow and metabolic abnormalities in Alzheimer's disease. *Ann Nucl Med* 15(2), 85-92. doi: 10.1007/BF02988596.
- Morrison, D.J., and Preston, T. (2016). Formation of short chain fatty acids by the gut microbiota and their impact on human metabolism. *Gut Microbes* 7(3), 189-200. doi: 10.1080/19490976.2015.1134082.
- Muir, E.R., Shen, Q., and Duong, T.Q. (2008). Cerebral blood flow MRI in mice using the cardiac-spin-labeling technique. *Magn Reson Med* 60(3), 744-748. doi: 10.1002/mrm.21721.
- Nagpal, R., Neth, B.J., Wang, S., Craft, S., and Yadav, H. (2019). Modified Mediterranean-ketogenic diet modulates gut microbiome and short-chain fatty acids in association with Alzheimer's disease markers in subjects with mild cognitive impairment. *EBioMedicine* 47, 529-542. doi: 10.1016/j.ebiom.2019.08.032.
- Napoli, E., Duenas, N., and Giulivi, C. (2014). Potential therapeutic use of the ketogenic diet in autism spectrum disorders. *Front Pediatr* 2, 69. doi: 10.3389/fped.2014.00069.
- Nguyen, T.T., Ta, Q.T.H., Nguyen, T.K.O., Nguyen, T.T.D., and Giau, V.V. (2020). Type 3 Diabetes and Its Role Implications in Alzheimer's Disease. *Int J Mol Sci* 21(9). doi: 10.3390/ijms21093165.
- Norwitz, N.G., Saif, N., Ariza, I.E., and Isaacson, R.S. (2021). Precision Nutrition for Alzheimer's Prevention in ApoE4 Carriers. *Nutrients* 13(4). doi: 10.3390/nu13041362.
- Paoli, A., Mancin, L., Bianco, A., Thomas, E., Mota, J.F., and Piccini, F. (2019). Ketogenic Diet and Microbiota: Friends or Enemies? *Genes (Basel)* 10(7). doi: 10.3390/genes10070534.
- Pistollato, F., Sumalla Cano, S., Elio, I., Masias Vergara, M., Giampieri, F., and Battino, M. (2016). Role of gut microbiota and nutrients in amyloid formation and pathogenesis of Alzheimer disease. *Nutr Rev* 74(10), 624-634. doi: 10.1093/nutrit/nuw023.
- Roher, A.E., Debbins, J.P., Malek-Ahmadi, M., Chen, K., Pipe, J.G., Maze, S., et al. (2012). Cerebral blood flow in Alzheimer's disease. *Vasc Health Risk Manag* 8, 599-611. doi: 10.2147/VHRM.S34874.
- Rusek, M., Pluta, R., Ulamek-Koziol, M., and Czuczwar, S.J. (2019). Ketogenic Diet in Alzheimer's Disease. *Int J Mol Sci* 20(16). doi: 10.3390/ijms20163892.
- Silva, Y.P., Bernardi, A., and Frozza, R.L. (2020). The Role of Short-Chain Fatty Acids From Gut Microbiota in Gut-Brain Communication. *Front Endocrinol (Lausanne)* 11, 25. doi: 10.3389/fendo.2020.00025.
- Tai, L.M., Thomas, R., Marottoli, F.M., Koster, K.P., Kanekiyo, T., Morris, A.W., et al. (2016). The role of APOE in cerebrovascular dysfunction. *Acta Neuropathol* 131(5), 709-723. doi: 10.1007/s00401-016-1547-z.
- Tran, T.T.T., Corsini, S., Kellingray, L., Hegarty, C., Le Gall, G., Narbad, A., et al. (2019). APOE genotype influences the gut microbiome structure and

- function in humans and mice: relevance for Alzheimer's disease pathophysiology. *FASEB J* 33(7), 8221-8231. doi: 10.1096/fj.201900071R.
- Wlodarek, D. (2019). Role of Ketogenic Diets in Neurodegenerative Diseases (Alzheimer's Disease and Parkinson's Disease). *Nutrients* 11(1). doi: 10.3390/nu11010169.
- Zajac, D.J., Green, S.J., Johnson, L.A., and Estus, S. (2022). APOE genetics influence murine gut microbiome. *Sci Rep* 12(1), 1906. doi: 10.1038/s41598-022-05763-1.
- Zhoa, Z., Lange, D., Voustianiouk, A., MacGrogan, D., Ho, L., Suh, J., et al. (2006). A ketogenic diet as a potential novel therapeutic intervention in amyotrophic lateral sclerosis. *BMC Neuroscience* 7. doi: <https://doi.org/10.1186/1471-2202-7-29>.



## VITA

### **Educational Institutions**

Vanderbilt University – Bachelor of Science in Neuroscience

University of Kentucky – Master of Science in Medical Science (in progress)

### **Professional Positions**

Senior Laboratory Technician (University of Kentucky, Sanders-Brown Center on Aging, Dr. Ai-Ling Lin)

Senior Laboratory Technician (University of Kentucky, Department of Physiology, Dr. Kenneth Campbell)

---

Andrew Yackzan

*(name of student)*